PNNL-32499

Storage Enabled Flexibility of Conventional Generation Assets (StorFlex)

November 30, 2021

Bilal Ahmad Bhatti
Ahmad Tbaileh
Sarmad Hanif
Saptarshi Bhattacharya
Jan Alam
Kyle Desomber

U.S. DEPARTMENT OF ENERGY
Prepared for the U.S. Department of Energy
Under contract DE-AC05-76RL01830

PACIFIC NORTHWEST NATIONAL LABORATORY
operated by
BATTELLE
for the
UNITED STATES DEPARTMENT OF ENERGY
under Contract DE-AC05-76RL01830

Printed in the United States of America

Available to DOE and DOE contractors from the
Office of Scientific and Technical Information,
P.O. Box 62, Oak Ridge, TN 37831-0062;
ph: (865) 576-8401
fax: (865) 576-5728
email: reports@adonis.osti.gov

Available to the public from the National Technical Information Service
5301 Shawnee Rd., Alexandria, VA 22312
ph: (800) 553-NTIS (6847)
email: orders@ntis.gov <https://www.ntis.gov/about>
Online ordering: http://www.ntis.gov

PNNL-32499

Storage Enabled Flexibility of Conventional Generation Assets (StorFlex)

November 30, 2021

Bilal Ahmad Bhatti
Jan Alam
Saptarshi Bhattacharya
Sarmad Hanif
Ahmad Tbaileh
Kyle Desomber

Prepared for
the U.S. Department of Energy
Under Contract DE-AC05-76RL01830

Pacific Northwest National Laboratory
Richland, Washington 99352

Abstract

The power systems have faced progressively more demanding operational requirements over the last two decades. Several factors contribute to these challenging operating conditions, including load growth, aging infrastructure, increasing penetrations of distributed energy resources (DERs), electrification of the economy, and policy initiatives such as decarbonization. The power system and its components must provide high operational flexibility to mitigate these challenges. For example, the proliferation of intermittent DERs such as wind and solar has increased the need for conventional generation assets like hydropower plants to respond to sudden load-generation imbalances. The higher flexibility requirements for hydropower plants cause more wear and tear, potentially shortening the useful lifespan of hydropower turbines. To reduce the need for hydropower plants to follow sudden changes in the dispatch signal, we investigate their combined operation with the energy storage systems (ESSs; "ESS-based hybridization").

Our analyses focuses on improving the lifespan of hydropower plants through ESS-based hybridization. Wear and tear on hydropower turbines (particularly Francis turbines) is modeled using a loss-of-life concept that is based on damage experienced by the turbine due to various cycles of operation. Then, we show that using ESSs to offset some of the high variation increases the remaining life of the hydropower plants. To demonstrate this, a few modeling tools were developed for this work: (1) a dynamic model for various components of the turbine and its governor; (2) a control strategy that assigns a slow-varying dispatch signal to a hydropower unit versus a fast-moving signal to ESS, such that the overall power request remains the same; and (3) models for the financial analysis to quantify the economic merits of such a framework.

We used the models we developed to analyze the dispatch pattern of an actual hydropower plant with a power output of 50 MW and a head height of 152 m. This work showed that ESS-based hybridization could extend the life of the hydropower plant by 5% on average. This extension in life was then used to estimate the economic benefit in terms of cost deferrals associated with hydropower plant maintenance and replacement: on average, $3.6 million. Sensitivity analysis with respect to the size of ESS and cost of turbines was performed to show the variation in benefits over the range of turbine costs and ESS sizes. Crucially, stacking damage reduction and lifetime extension with other ESS value streams such as providing ancillary services could substantially increase the financial benefits of ESS-based hybridization. The higher costs associated with ESS of appropriate size would make more financial sense when multiple value streams are stacked and co-optimized to extract the maximum benefit. This dimension will be explored in future work.

Acronyms and Abbreviations

BEP	best efficiency point
DER	distributed energy resource
ESS	energy storage system
EWEB	Eugene Water and Electric Board
Li	lithium
PID	proportional integral derivative
PSH	Pumped Storage Hydro
p.u.	per unit
PV	photovoltaic
T&D	Transmission and Distribution
TRL	technical readiness level

Acknowledgments

This material is based upon work supported by the U.S. Department of Energy's (DOE) Office of Electricity Energy Storage program through the program director Dr. Imre Gyuk. We thank the Eugene Water and Electric Board, Eugene, Oregon, for providing relevant data and information.

Contents

Abstract iv
Acronyms and Abbreviations v
Acknowledgments vi

1.0 Introduction 1
1.1 Motivation and Challenges 2
1.2 Proposed Framework 3

2.0 Modeling and Analysis 5
2.1 Loss-of-Life Models 5
2.2 Hydro Turbine and Governor Modeling 9
2.3 Hybridization Control Strategy 10
2.4 ESS Modeling 14
2.5 Economic Modeling 15

3.0 Simulation and Case Studies 17
3.1 Base Case 18
3.2 ESS-Based Hybridization with Fixed Battery size 22
3.3 Sensitivity Analysis 26
3.4 Economic Analysis 27
3.5 Discussion of Results 29

4.0 Conclusion and Recommendations 31

5.0 Appendix 33

6.0 References 34

Figures

1 PSH dominates the installed ESS capacity making up about 98% of the installed ESS capacity. Li-ion is second in this list and is among the rapidly growing technologies. 1

2 New grid-connected ESS capacity installed each year and future projection. 1

3 Conceptual view of the proposed hybridization framework. 4

4 Relationship between number of cycles to failure with stress experienced by the material [40]. The y-axis shows the stress level that a material can endure for a corresponding number of cycles (x-axis). Higher stress reduces the number of cycles a material can endure before it fails. 6

5 Overview of the loss-of-life calculation procedure. 8

6 Overview of the simplified governor and turbine model [22]. 9

7 Demonstration of the modeled dynamics of governor and turbine; x-axis for all plots is the time in seconds and y-axis is the p.u. of the respective base quantity. 10

8 Hybrid controller creates two separate signals for the ESS and the hydropower unit. When the ESS is not able to dispatch (i.e., is fully charged or discharged), then the additional dispatch is picked up by the hydropower unit. 11

9 Modeling ESS-based hybridization as a closed-loop system. 12

10 Detailed model of the ESS-based hybridization controller. 12

11 Frequency response of LF-1. 13

12 Frequency response of LF-2. 14

13 Power output of unit-2 for one month. The unit operation in the low part load region and frequent shutdowns/startups cause wear and tear. 18

14 Setup for the base case simulation. EWEB's original dispatch signal drives the hydro turbine unit to provide an estimate of the baseline damage. 19

15 State variables in the base case simulation. 19

16 Electrical power (Pe), mechanical power (Pm), and gate position (G) follow the reference signal delayed by the inertia of the machine. 20

17 Load-generation imbalance to simulate the real-world loading conditions. 20

18 Breakdown of the damage incurred in base case simulation. 21

19 Ramp-limited, slowly varying dispatch signal for hydro turbine generator as generated by hybrid controller. 23

20 Energy-neutral, rapidly changing dispatch signal as generated by hybrid controller. . . 24

21 State variables in the hybrid case simulation. 24

22 Comparing damage in hybrid case with the base case. 25

23 Comparing damage breakdown in hybrid case with the base case. 25

24 Percent damage reduction due to hybridization expressed as a function of normalized battery peak power and normalized energy capacity. 26

25 Total Benefit from avoided maintenance and total benefit from investment deferral. . . 28

26 Total benefit from ESS-based hybridization over a range of turbine replacement costs and ESS sizes. 28

27 Benefit-to-cost ratio as a function of turbine replacement cost and ESS size. 29
28 EWEB recommendations for operating generating units at the Carmen facility. 33

Tables

1 Worldwide installed capacity of ESS. 2
2 Specifications of generating units at EWEB's Carmen-Smith hydropower facility. 17
3 Damage classification categories defined for unit-2 based on operational recommendations from EWEB. 17
4 Generator parameters 21
5 Turbine parameters 22
6 Parameters for the hybrid controller. 22
7 Economic analysis parameters. 27

1.0 Introduction

Energy storage systems (ESSs) can provide flexibility and multiple ancillary services to the electric grid. Their deployment continues to grow worldwide [32], and capital costs are decreasing due to economies of scale. Some technologies, such as lithium (Li)-ion batteries, have seen a significant decrease in cost over the last decade, with the cost predicted to be halved by 2030 [12] as compared to 2019 costs. ESSs are often deployed to mitigate the inherent variability and uncertainty associated with distributed energy resources (DERs) such as solar photovoltaic (PV) generation. However, this text specifically refers to the grid-connected ESSs. Table 1 shows the breakdown of total grid-connected ESS capacity worldwide in megawatts (MW). The installed capacity is dominated by pumped storage hydro (PSH) followed by Li-ion technology. In fact, 97.6% of the installed ESS capacity consists of PSH as shown in Figure 1, which also shows the breakdown of installed capacity among technologies other than PSH. The grid-connected ESS capacity is projected to increase globally. Within the United States, annual ESS deployment is expected to quadruple from 2019 to 2022 [12], [32], as shown in Figure 2.

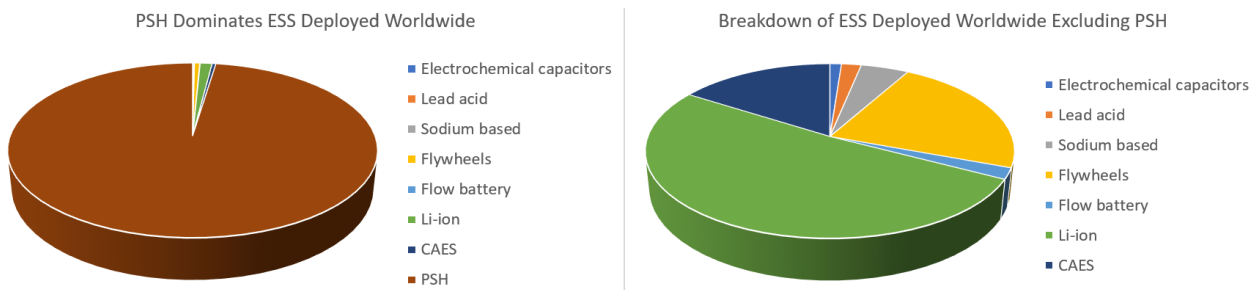

Figure 1. PSH dominates the installed ESS capacity making up about 98% of the installed ESS capacity. Li-ion is second in this list and is among the rapidly growing technologies.

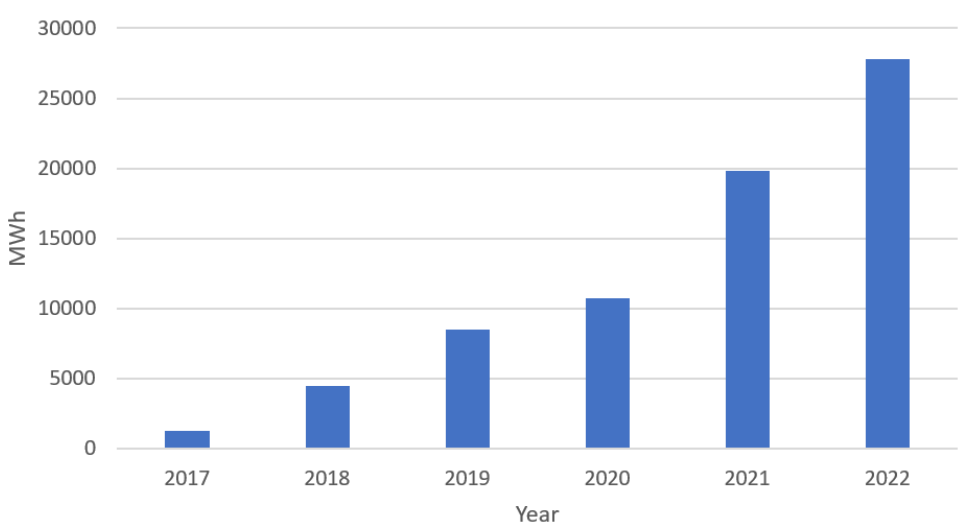

Figure 2. New grid-connected ESS capacity installed each year and future projection.

Table 1. Worldwide installed capacity of ESS.

Technology Type	MW
Lead acid	84
Compressed-air energy storage	660
PSH	169,557
Flywheels	931
Flow battery	85
Electrochemical capacitors	49
Sodium-based battery	204
Li-ion battery	2122
Total	173,692

(a) Installed capacity includes systems that are currently offline for maintenance.

(b) Source: DOE OE Global Energy Storage Database

(c) The numbers should be considered approximate because some records are unverified.

1.1 Motivation and Challenges

One of the significant advantage of ESSs compared to conventional generators is their ability to provide operational flexibility to the grid. This flexibility is offered in the form of multiple behind-the-meter or front-of-the-meter services that can be stacked and co-optimized for maximum benefit. The benefit streams and services that have been explored in the literature have been strongly related to the Transmission and Distribution (T&D) sector. Examples of such services include backup power, demand charge reduction, frequency regulation, and energy arbitrage. The true potential of ESS extends beyond T&D; however, its benefit streams in other sectors such as generation are understudied.

A promising value stream that can be extracted from ESS is the combined operation of ESS with conventional generation assets, referred to in this report as ESS-based hybridization. Note that this is distinct from either combining different energy storage types to work as one source [14] or connecting different voltages (e.g., AC and DC) to ESS interconnections [23] (other schemes also referred to in the literature as “hybrid ESS”).

This report does not address the combined operation of ESS with variable renewable resources such as PV and wind turbines, where ESS is used to complement the variations in output power to produce a near-constant output [19] – another common technology referred as “hybrid ESS”. In particular, this report looks at the combined operation of ESS with hydroelectric turbine generators. Under such a setup, the fast ramping capability and flexibility of ESSs can be leveraged to offset the slow ramping of hydropower units. The combined operation of ESS and hydropower assets provides a unique opportunity to mix and match the desired characteristics of both assets, thus yielding economic and operational benefits.

There has been some work in assigning fast and slow ramping signals to ESS and thermal generation, respectively [21]; however, the overall techno-economic benefit of ESS hybridization

with conventional technologies such as hydropower has been understudied. This is important for two reasons. First, hydropower plants are now being required to provide a higher level of flexibility than they have conventionally provided. Second, hydropower is considered an inexpensive renewable energy resource. The wear and tear on hydropower plants incurred by providing highly variable power may result in plants needing major upgrades and facing long shutdown durations, moving them from an inexpensive resource to an expensive one. There are industry solutions targeted at analyzing such operations (see the hybrid solution provided by vendors in [13]), but these solutions are not available to the plant operator to modify based on their individual needs, adding to the overall cost of hydropower plant operation.

Before discussing the framework in detail, let us look at some of the challenges that still exist to the widespread adoption of ESS for the grid. These challenges are summarized as follows [5, 4, 30, 2, 29]:

- Despite the predicted decrease in costs, ESS technologies bear a high initial cost of deployment.
- On top of the initial costs, there are additional costs associated with the safety and testing requirements for nascent technologies.
- ESS requires a power electronic interface for grid integration, which must be developed while adhering to grid-related safety protocols, resulting in additional costs.
- Uncertainties are associated with regulatory and policy aspects that create reluctance among investors of such projects.
- Utilities have generally shown a reluctance to adopt new tools and tend to lean on established practices; therefore, it is critical to develop ESS platforms that integrate effectively with existing tools.

1.2 Proposed Framework

To understand the potential of achieving better value from grid assets through ESS-based hybridization, a proof-of-concept framework is developed for evaluating and enabling the benefit of ESS-based hybridization. The conceptual view of the framework is shown in Figure 3. The ESS-based hybridization is enabled by a hybrid controller that modifies the operation of the ESS and the conventional asset. Then, multiple value streams are captured to quantify the value of hybridization. The first is the value from avoiding damage (due to wear and tear). The prerequisites for this value stream are the loss-of-life and damage models for conventional assets. The second value stream involves the operational constraints on the asset, such as load profiles and avoiding certain operational zones. The first two value streams relate directly to maintenance requests because they result in wear and tear of the asset. The framework is flexible, so other value streams can be stacked on top of the existing streams. All the value streams are monetized to calculate the benefit of the ESS-based hybridization. The key studies performed in this work are as follows:

- Analyze loss of life in a hydropower generator when it operates in combination with the ESS.
- Study a hybrid controller that relieves the hydropower generator from high-load fluctuations and attempts to extend its lifetime by reducing wear and tear.

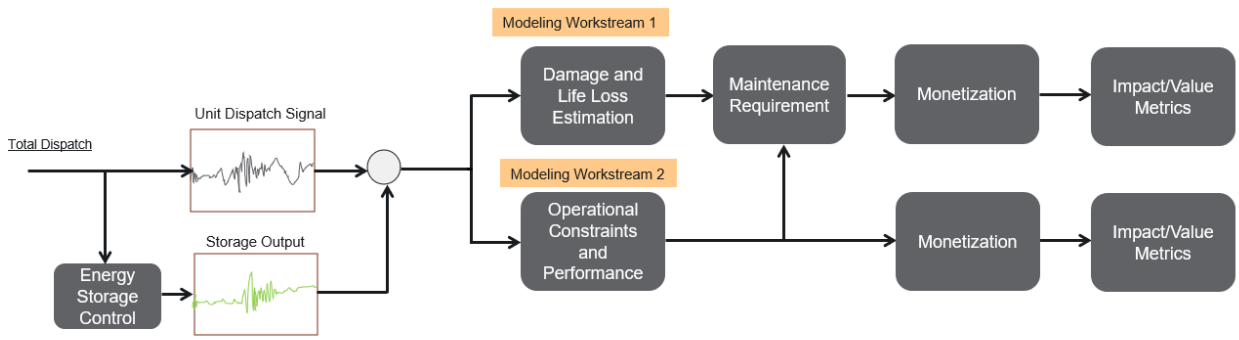

Figure 3. Conceptual view of the proposed hybridization framework.

- Analyze and quantify multiple value streams, such as benefits of reducing maintenance costs and deferring investments (for replacements) due to lifetime extension, resulting from ESS-based hybridization.

The rest of the report is organized as follows. Section 2.0 describes the models deployed in this work. Case studies and simulation results are analyzed in Section 3.0, followed by conclusions and recommendations in Section 4.0.

2.0 Modeling and Analysis

This section describes the models deployed for analyzing ESS-based hybridization. First, we introduce the loss-of-life modeling adopted in this report, followed by the governor and turbine models of the hydropower plant units. We then introduce the control methodology deployed to achieve the ESS-based hybridization. The section concludes with the ESS modeling and economic framework to analyze the benefits of the proposed ESS-based hybridization.

2.1 Loss-of-Life Models

The operation of a turbine is expected to result in a certain lifespan for the turbine; wear and tear due to various operating conditions accumulate and eventually lead to the replacement of the turbine. A loss-of-life model can help quantify how much damage a turbine experiences given its operating conditions (e.g., loading/cycling). This section explains the procedure for obtaining such a loss of life model for the turbine. There are three main sets of ideas to calculate turbine fatigue due to various operating conditions [25].

The first set of research in this area is through the development of a maintenance and deterioration model of individual plant components [44, 10], expressed through various system states and transition probability. For example, one can model states to describe various operational capabilities of the plant (state 1 – fully operational, state 2 – slightly degraded, state 3 – moderately degraded, and state 4 – critical condition). Then, based on transition probability, the states converge to failure. The second research theme uses cumulative damage theory based on statistical and physical relationships of the underlying components of the hydropower plant [18, 28, 36, 1, 17]. The third research theme is related to detailed modeling of turbine components and its deterioration using the finite element method or computational fluid dynamics [8].

In this report, we deploy cumulative damage theory for calculating damage to the turbine due to fatigue it experiences in following a particular dispatch signal. The main reason for adopting this method is that it provides a tradeoff between a detailed physics-based model [8] and a purely statistics-based model [44].

Before explaining the loss-of-life model, we present the rationale for damage calculation and approximation of the affected lifetime of the turbine. We assume the hydropower plant has serially connected components, which is sufficient to only evaluate the critical part, which is assumed to be the turbine and specifically its runner. This is because failure in the turbine occurs at the area with the largest stresses, so it is sufficient to only analyze the runner of the turbine [40]. The fatigue analysis can then be performed to give the remaining lifetime of the turbine.

To evaluate the fatigue damage, the Palmgren–Miner model proposes the following model [18]:

$$D = \sum_{i}^{k} D_i = \sum_{i}^{k} \frac{n_i}{N_i(\Delta\sigma)} \tag{1}$$

where D is defined as the cumulative linear summarized damages for k stress events. The number of load cycles at a given stress level is n_i, and N_i is the maximum number of load cycles given by the S-N (stress to number of cycles) curve at that particular load. The changes in stress are represented by $\Delta\sigma$. An example of S-N curve is given in Figure 4. From Equation (1), the principle of the model is such that once the value of D reaches 1, the component is assumed to be failed. Hence, the remaining life after stress events can be calculated as:

$$R = 1 - \sum_{i}^{k} D_i. \tag{2}$$

An alternate expression for calculating remaining life is:

$$R = 1 - \sum_{i}^{k} D_{i,fatigue} - \sum_{i}^{k} D_{i,static}, \tag{3}$$

which is composed of the static and fatigued components of the stress. This definition is similar to Equation (3), but decomposed into types of stress.

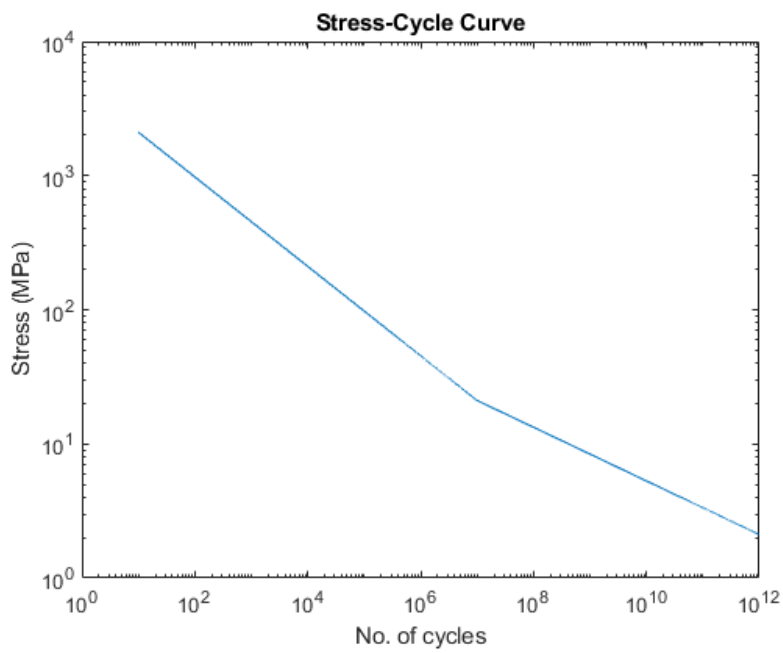

Figure 4. Relationship between number of cycles to failure with stress experienced by the material [40]. The y-axis shows the stress level that a material can endure for a corresponding number of cycles (x-axis). Higher stress reduces the number of cycles a material can endure before it fails.

From the above, it can be seen that estimating the (1) operating patterns which yield significant stress patterns and (2) calculation of stress on the equipment are the main components of the loss-of-life estimation using the fatigue damage calculation method. For the purpose of analyzing hydropower plant turbine efficiency, the usual patterns of its operation are divided into [39]:

1. Startup [cycle/day]: Each cycle is counted as the number of times in a day when the turbine goes from no-load (shutdown) operation to achieve nominal synchronization speed.

2. Speed no-load [%]: Measured as fractions of time when the turbine is spinning without being synchronized to the grid.

3. Low part load [%]: Percentage of time the turbine delivers low part load.

4. Part load [%]: Percentage of time the turbine delivers partial load.

5. Best efficiency point (BEP) [%]: Percentage of time the turbine delivers power with most efficiency.

6. High load [%]: Percentage of time the turbine delivers power at a rate higher than it is designed for.

The above operating regimes are determined either through observations or rules or ideally through a hill chart [24]. In this project, dispatch data for a hydropower plant (in MW) was available, along with a guide to avoid areas of operation (as shown in Figure 28). The project used this information to draw on a few simplifications as follows:

- First, percentage operation of speed no-load pattern was merged into the low part load operating pattern. This is because the relative damage due to speed no-load has been shown to be comparable to low part load [27]. As the low part load operation is classified as the operation regime where guide vanes are partially opened and flow rates are low, we assume lower production regions of the Appendix Figure 28 are the low part load regions. The last simplification is assumed to be made in figuring out the operating pattern of BEP. This is usually obtained using a hill chart [24], which combines the functions of head, flow rate, and rotational speed to demonstrate the BEPs. However, due to missing information on these parameters and general guidance of the operator as given in Figure 28, we assume the power output around the green region as the BEP pattern, and higher and lower power generation as high load and part load, respectively.

- Apart from simplification on the operating pattern extraction from the given data, the other simplification is made in terms of stress calculation due to the inflicted operating patterns. The first estimation is done on the material parameters of "welded along load-carrying joints", taken from [40], for a common high-head Francis turbine material. The second estimation is on the effective stress experienced by the component during the operating patterns (e.g., part load, BEP). There are three methods of obtaining the mean stress: through experimental procedure; by modeling a digital equivalent of the component in a high-accuracy simulator (e.g., ANSYS [41]); or by using the analytical methods. Advantages and disadvantages of these methods are given in [40]. For a turbine similar to the size of the hydropower plant studied in this report, mean stress measurements have been published in the literature for various operating conditions. We use and correct these measurements to get the effective stress, s_{eff}, for different operating conditions as follows:

$$s_{eff} = s^{amp} \cdot \left(\frac{UTS}{UTS - s^{mean}} \right) \cdot 10^6 \tag{4}$$

  where s^{amp} is the amplitude stress value, s^{mean} is the mean stress value, and $UTS = 910 \cdot 10^6$ is the yield strength [15]. Finally, the effective stress for the start-stop condition is adjusted to be 3 times at BEP, as experimental evidence shows that the guide vanes are opened 2.5 to 3 times during startup as compared to BEP. Hence, this procedure correlates the guide vane opening with effective stress on the turbine runner.

- The final adjustments are performed on the frequency measurement at different operating points. The frequency measurements during operating patterns of part load (f^m_{pl}), low part

load (f^m_{lpl}), BEP (f^m_{bep}), and high load f^m_{hl} are adjusted as:

$$f_{lpl} = \frac{f^m_{lpl}}{3.6} + f^m_{lpl} \cdot gv \tag{5a}$$

$$f_{pl} = \frac{f^m_{pl}}{3.6} + f^m_{pl} \cdot gv \tag{5b}$$

$$f_{bep} = f^m_{bep} \cdot gv \tag{5c}$$

$$f_{hl} = f^m_{hl} \cdot gv \tag{5d}$$

where gv are the number of guide vanes multiplied to convert the turbine frequency into the total rotational velocity of the fluid flowing through the runner. The factor 3.6 is due to the effect called as Rheingans frequency [40]. The frequency for one startup is taken as 20 times the BEP, as demonstrated in the experiments conducted in [40].

With the above-mentioned simplifications, the overview of the main inputs, calculation procedure, and the final output is presented in Figure 5.

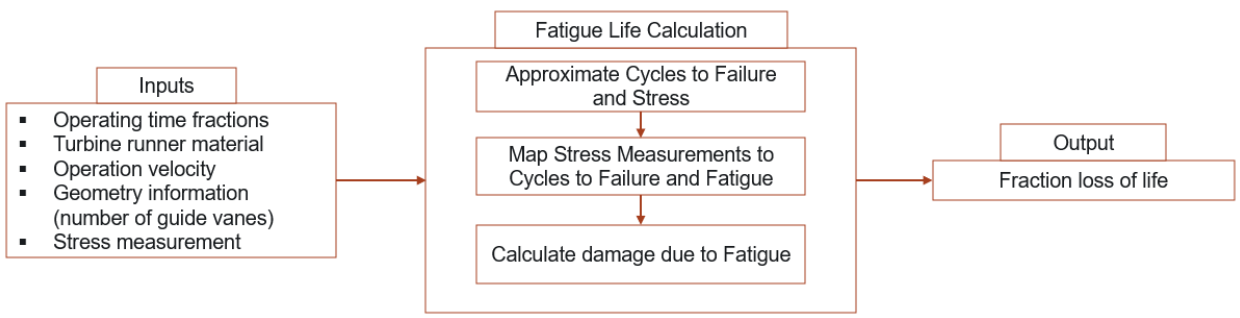

Figure 5. Overview of the loss-of-life calculation procedure.

To circumvent issues of data availability, the method presented above provides alternatives to approximate variables and uses the established relationships of S-N curves from the literature of the same turbine type. However, some methods in the literature provide further simplification of damage calculations. First is the work in [26], where the authors empirically found coefficients that correlate damage to the equipment based on the historical operation and degradation in performance. For example, if a turbine produced 20% less power output for the same input dispatch signal, then a simple damage calculated for the turbine in its experienced life is 20%, if not maintained or renovated. Then the trajectory of obtaining final damage of 20% was fitted to the time series data and either an exponential or linear curve is obtained to explain the relationship. Second is the experimental relationships between power output and the dynamic and static stresses experienced by the turbine as a whole [43]. With this method, measurements of variables, such as experienced stress of the components or frequency of the system, can be avoided and the delivered power can directly be correlated to the stress experienced by the turbine.

Note that the loss-of-life calculation needs to be augmented with the operation of the hydropower plant. (1) The frequency measurements for various operating points can be taken from the modeled plant operation[1]. (2) The dynamics associated with different components of the grid may be modeled and a realistic impact on the operation may be obtained due to different operating patterns. (3) This can serve as the framework for testing various control

[1]Since there was no head or flow information available, we omit the frequency measurements from the dynamic model and use the above-simplified relationships to obtain the damage calculations.

strategies. Any combination of these three reasons warrant a dynamic hydro turbine and governor model, which is explained next.

2.2 Hydro Turbine and Governor Modeling

In Equation (6), variables $[\dot{x}_{g1}, \dot{x}_{g2}, \dot{x}_{g3}, \dot{x}_{g4}]$ are state variables used to model gate position G and mechanical power P_m. The system of differential equations in (6) is initialized using the steady-state operating conditions $\omega_{ref} = \omega$ and by making all differential variables equal to zero. The differential equations are solved using a fourth-order Runge–Kutta method [6]. More information on the derivation of the model and the time constants adopted can be found in [22]. For the sake of brevity, the generator is not modeled in detail.

$$\dot{x}_{g1} = \left(\frac{1}{T_p}(\omega_{ref} - \omega) + (\sigma K_p - 1)x_{g1} - \sigma x_{g2} + \sigma P_{ref}\right) \tag{6a}$$

$$\dot{x}_{g2} = K_i x_{g1} \tag{6b}$$

$$\dot{x}_{g3} = v = \begin{cases} \frac{1}{T_g}(-K_p x_{g1} + x_{g2} - G) & \text{if } v_{max} \geq \frac{1}{T_g}(-K_p x_{g1} + x_{g2} - x_{g3}) \geq v_{min} \\ v_{max} & \text{if } v_{max} < \frac{1}{T_g}(-K_p x_{g1} + x_{g2} - G) \\ v_{min} & \text{if } v_{min} > \frac{1}{T_g}(-K_p x_{g1} + x_{g2} - G) \end{cases} \tag{6c}$$

$$\dot{x}_{g4} = \frac{1}{T_w}\left(1 - \left(\frac{x_{g4}}{G}\right)^2\right) \tag{6d}$$

$$G = \begin{cases} x_{g3} & \text{if } G_{max} \geq x_{g3} \geq G_{min} \\ G_{max} & \text{if } G_{max} < x_{g3} \\ G_{min} & \text{if } G_{min} > x_{g3} \end{cases} \tag{6e}$$

$$P_m = x_{g4}\left(\frac{x_{g4}}{G}\right)^2 \tag{6f}$$

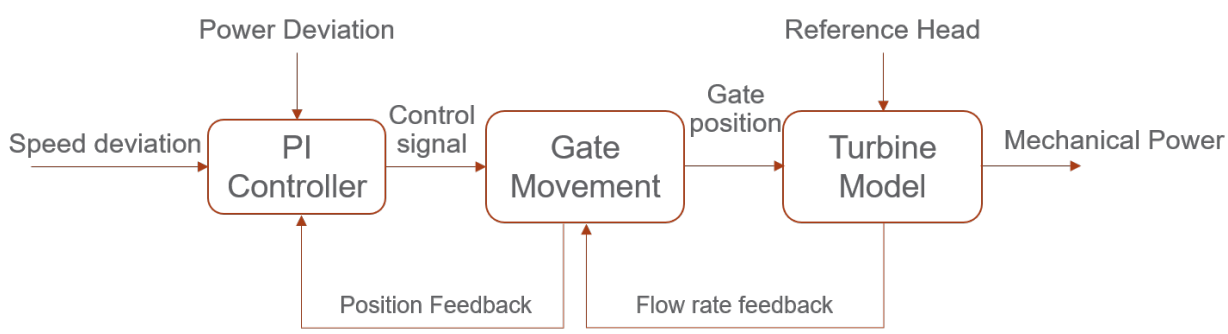

Figure 6. Overview of the simplified governor and turbine model [22].

Figure 7 shows the dynamics of the modeled system of Equation (6). The variable p_{ref} is the reference power imposed on the governor-turbine model, i.e., the input of the model. The reference speed of the turbine is set to be 60 Hz or 1 per unit (p.u.). The resultant dynamics in Figure 7 are then obtained as the turbine tries to follow the reference power. Note that the gate G opens and closes to follow power reference values and generates proportional mechanical power p_m from the turbine. As mentioned earlier, the electrical power p_e is not modeled separately, so $p_m = p_e$ and that is the final power delivered by the turbine.

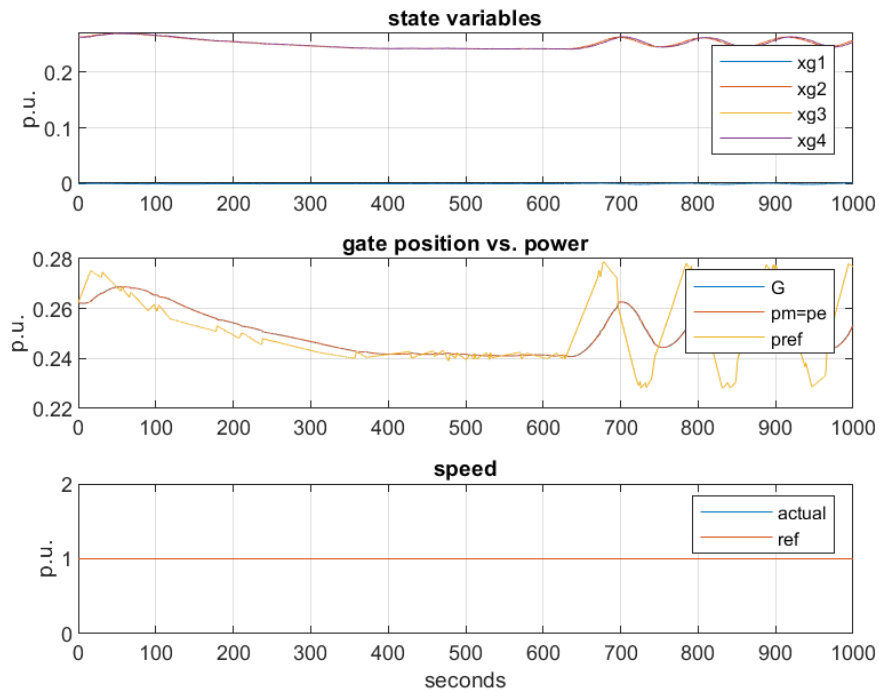

Figure 7. Demonstration of the modeled dynamics of governor and turbine; x-axis for all plots is the time in seconds and y-axis is the p.u. of the respective base quantity.

2.3 Hybridization Control Strategy

This section discusses a control strategy that reduces the damage during the hydropower unit operation by dividing the burden of variable dispatch between the hydropower unit and the ESS. This is a nascent area of research, and most of the work in the past has focused on relieving the burden on the thermal units. Thermal units are typically not capable of ramping up or down quickly; therefore, they cannot follow a rapidly fluctuating dispatch signal. In [9], [37], the highest fluctuations from the dispatch signal are removed and the modified smooth signal is used to dispatch the thermal units. Similarly, a separating filter is proposed in [21] that decomposes the dispatch signal into a high-frequency and a low-frequency signal. The high-frequency signal is followed by the ESS, and the low-frequency signal is followed by the thermal units. The authors in [35] proposed that the hydro units can relieve the thermal units by picking up the high fluctuations, leaving the slow load variations for the thermal units to follow. A dead-band-based approach for the thermal units was proposed in [38] that relied on batteries to follow the rapidly varying load changes. A similar study in [20] employed a battery for dispatching the fast regulation signal. In a generic approach [16], PJM (a regional U.S. transmission organization) discussed a method to derive fast and slow ramping signals for fast and slow ramping resources, respectively.

The hybridization control strategy discussed in this text dispatches the ESS to reduce the damage on the hydropower unit and therefore extend its lifetime. It is based on a hybrid controller that divides the utility dispatch signal into two signals. As shown in Figure 8, the two signals are separately fed to the ESS and hydro unit. The controller assumes the role of dividing the load burden between the two assets such that:

- The life of the conventional asset (i.e, the hydro turbine generator) is prolonged. This is achieved by assigning a slow-varying dispatch signal to the hydro units to avoid wear and tear.
- The rapidly fluctuating dispatch signal is fed to the ESS model. However, the actual ESS output may differ, because ESS is a power- and energy-limited resource. Therefore, the ESS state of charge (SOC) and power limit may not allow (or may partially allow) it to follow the dispatch signal. In such scenarios, the additional dispatch burden must be picked up by the turbine, because the dispatch directive from the utility must be met. In the physical system, this might be achieved by providing a correction input to the turbine governor based on the ESS state.
- Combined output from the hydro turbine generator and ESS should follow the dispatch signal; in other words, it should mirror the output of the conventional asset operating by itself.
- The ESS signal is required to be energy neutral. This minimizes the violation of the SOC constraints. The energy neutrality implies that the total energy discharged over a period equals (plus or minus some tolerance) the total energy charged.

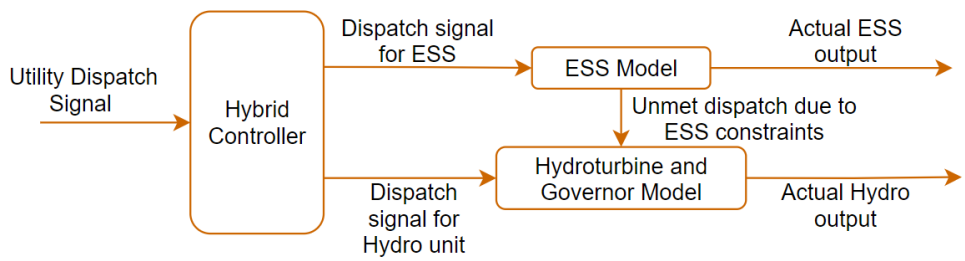

Figure 8. Hybrid controller creates two separate signals for the ESS and the hydropower unit. When the ESS is not able to dispatch (i.e., is fully charged or discharged), then the additional dispatch is picked up by the hydropower unit.

The hybrid ESS system is modeled in a closed-loop, as shown in figure 9. The dispatch signal from the utility is fed to the hybrid controller that splits it up into two dispatch signals (i.e., R_g for hydro turbine generator and R_{es} for ESS). The two signals are sent to their respective dispatch controllers which translate the signals into reference power signals for the hydro turbine generator and ESS. The hydro turbine generator system is modeled in three parts (governor, turbine, and synchronous generator). The turbine governor takes the error frequency signal ω_{ref} - ω as input and translates it into a gate signal for the turbine. The turbine translates the gate signal into mechanical power that is finally converted by the generator into electrical power P_g. In parallel, the ESS model converts the dispatch signal into electrical power from energy storage P_{es}. The two powers are combined at the point of common coupling and fed to the grid model. To model real-time changes in load–generation balance, a disturbance signal is generated and added. The grid model generates the frequency that is used as the feedback signal for the turbine control.

The input to the controller is the dispatch signal from the utility. Usually, these signals are based on real-time load-generation imbalance. The utilities aim to correct this imbalance by dispatching the generation assets in line with these signals. The individual building blocks of the controller shown in Figure 10 perform the following tasks:

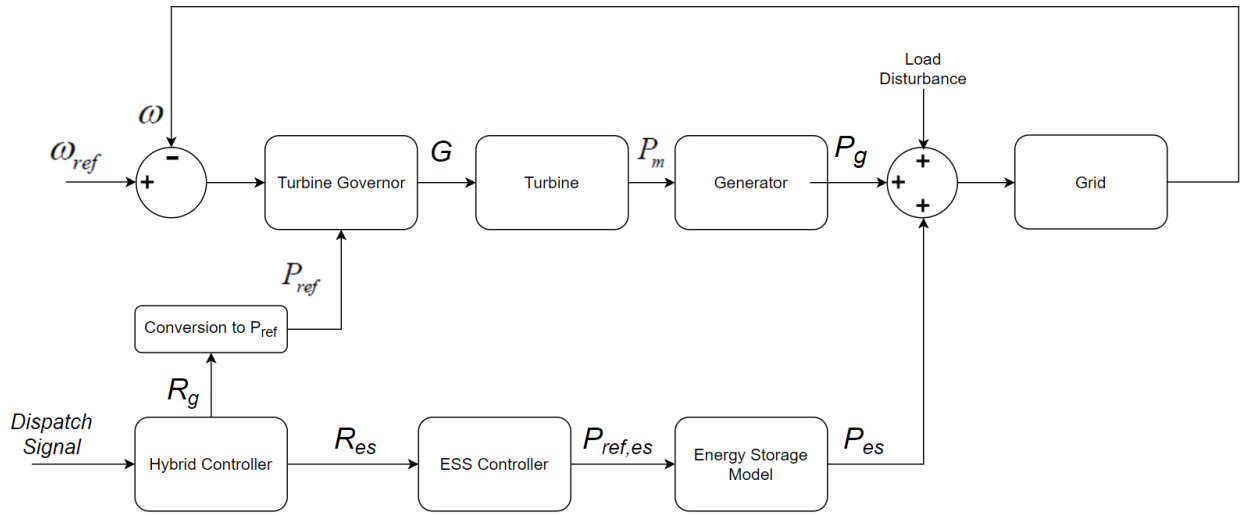

Legend

R_{es} = Energy Neutral, high frequency Dispatch signal
R_g = low frequency Dispatch signal
P_{ref} = Power Setpoint for turbine governor
$P_{ref,es}$ = Power Setpoint for energy storage

ω_{ref} = Frequency setpoint
ω = Measured Frequency
G = Gate position
P_m = Mechanical Power from turbine
P_g = Electrical Power from generator

P_{es} = Power output from ES

Figure 9. Modeling ESS-based hybridization as a closed-loop system.

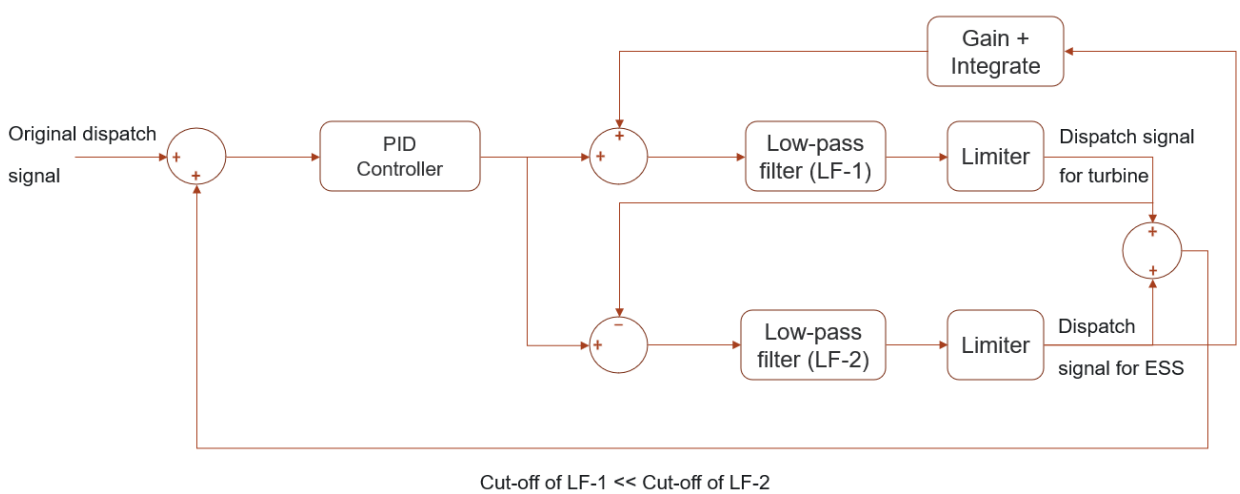

Figure 10. Detailed model of the ESS-based hybridization controller.

- The proportional-integral-derivative (PID) controller reduces the error between the control signal and actual power output (combined output of ESS and hydro turbine generator). The PID gains of the controller can be configured to force the error toward zero.
- The low pass filter-1 (LF-1) has a higher time constant (compared to LF-2) and thus permits the low-frequency content of the original signal to pass through it.
- The other low pass filter (LF-2) is fed with the difference of the error and the output signal of the LF-1. The time constant of LF-2 is smaller than the time constant of LF-1, so it generates a high-frequency signal. Figure 11 and Figure 12 show the frequency response of LF-1

and LF-2 with time constants of 150 and 6 [16] respectively. It can be seen that the cut-off frequency of LF-1 is much smaller than that of LF-2. Note that the time constants of both filters are configurable.

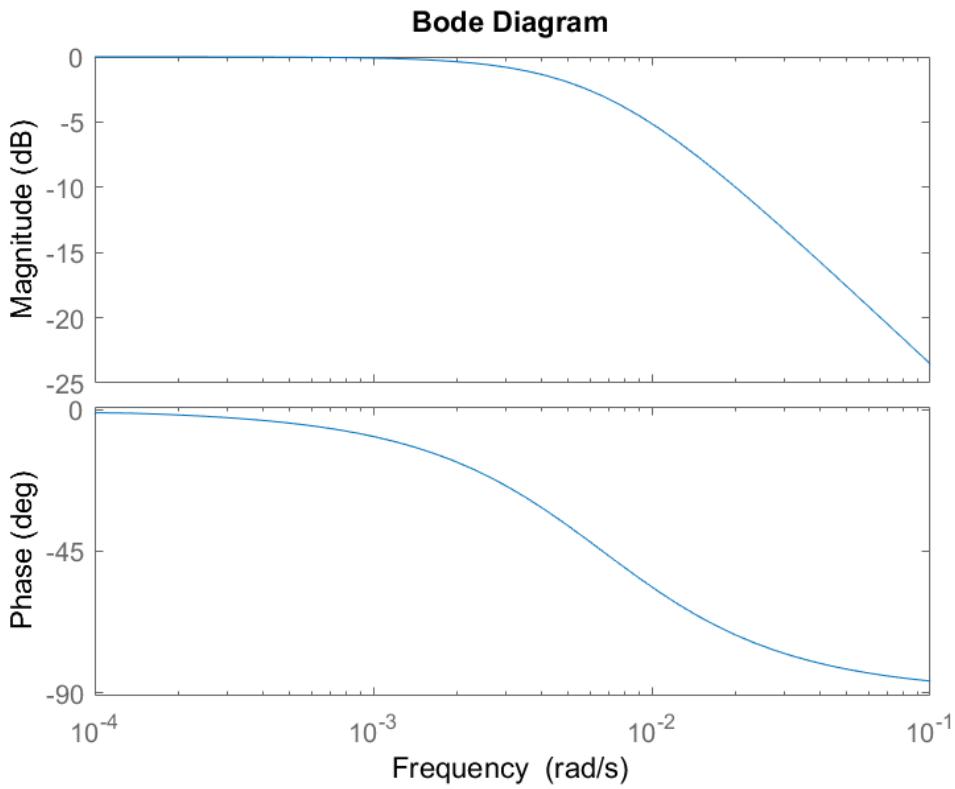

Figure 11. Frequency response of LF-1.

- The limiter's floor or ceil of the signal depending on the configured minimum or maximum value. They can be deployed to avoid certain regions of operation of the hydro turbine generator. These operation regions can be specified either through system knowledge or explicit modeling of low part load, part load, or high load, and are detrimental to the life of the turbine. For example, low part loads are often encountered during off-peak periods or times of the day. These blocks are also used to enforce the power constraints of the ESS.

- The Gain+Integrate block enforces energy neutrality, integrates the dispatch signal for ESS to maintain a sense of ESS SOC, and reverses the direction of the dispatch signal at regular intervals. This concept is similar to the one described in [16].

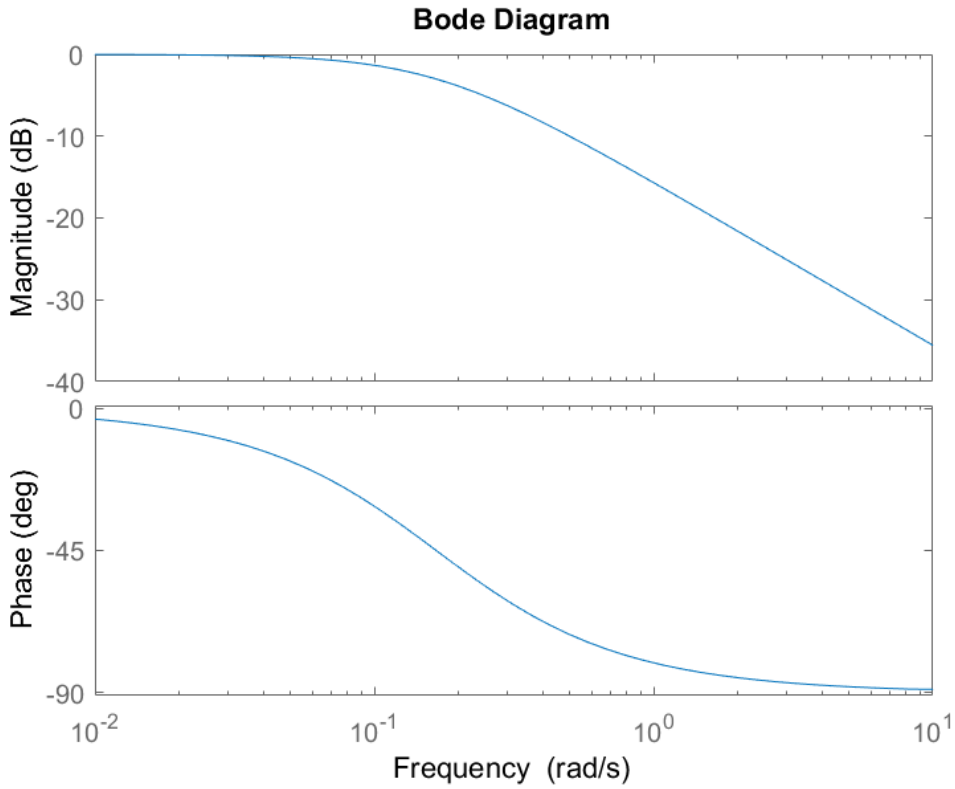

Figure 12. Frequency response of LF-2.

2.4 ESS Modeling

To realize ESS behavior, a generic, linear model is developed for the ESS. It maintains the SOC by using coulomb counting (a linear approach) and enforces charging and discharging efficiencies. The ESS constraints are listed as follows [7]:

$$0 < P_t^{ES\pm} < P_{max}^{ES\pm}, \qquad \forall t \tag{7}$$

$$SOC_{min} < SOC_t < SOC_{max}, \qquad \forall t \tag{8}$$

$$SOC_{t+1} = \begin{cases} SOC_t + \frac{(P_t^{ES-})\cdot\delta t}{60\cdot\epsilon_c}, & \text{if } charging \\ SOC_t - \frac{(P_t^{ES+})\cdot\delta t}{60\cdot\epsilon_d}, & \text{if } discharging \end{cases} \tag{9}$$

where P_t^{ES-} and P_t^{ES+} denote the ESS power output in MW during charging and discharging, respectively. In Equation (7), $P_{max}^{ES\pm}$ denotes the power limits of the ESS. Similarly, the SOC constraint is enforced by Equation (8) as SOC_{min}, SOC_{max}, and SOC_t denote the minimum, maximum, and current SOC respectively. The coulomb counting is implemented as in Equation (9), where battery SOC (in MWh) is incremented or decremented based on battery state. The ϵ_c and ϵ_d denote the charge and discharge efficiencies, whereas δt represents the incremental time interval (i.e., $\delta t = (t+1) - t$).

2.5 Economic Modeling

To analyze the techno-economic aspect of the hybrid operation, monetization of benefits from ESS-based hybridization is required. To this end, a simplified maintenance cost model is developed for the hydro turbine generator as follows.

- Looking at real-world maintenance data, the annual maintenance cost C_y^{mt} is modeled as 1% [33] of the turbine replacement cost C_{tot}^r. The cost is assumed to increase linearly with the total damage D incurred in the turbine:

$$C_y^{mt} = D \cdot C_{tot}^r \cdot \frac{1}{100} \tag{10}$$

- The total annual cost C_y becomes:

$$C_y = C_y^{mt} \tag{11}$$

- By using the annual cost in year-1 of operation and assuming an inflation rate (IR), the future annual costs are computed for each year of the lifetime of the hydro turbine generator. Then, for each year, a future annual benefit B_{fut}^i is calculated by taking a difference of the two annual costs, i.e., the cost in the base case $C_{fut,base}^i$ and the cost in the hybrid operation case $C_{fut,ess}^i$.

$$C_{fut}^i = C_y \cdot (1 + IR)^i \tag{12}$$

$$B_{fut}^i = C_{fut,base}^i - C_{fut,ess}^i \tag{13}$$

- Then, assuming a discount rate DR, the future benefit values are converted into present benefit values and summed over total life L_{tot} to yield the Net Present Value (NPV) of the benefit due to maintenance avoided B_{NPV}.

$$B_{NPV} = \sum_{i}^{L_{tot}} \frac{B_{fut}^i}{(1 + DR)^i} \tag{14}$$

- Next, to calculate benefit due to investment deferral B_{def}, investment deferral years y_{def} are calculated from the life removed in the base case L_{base}^{remov} and the life removed in the ESS-based hybrid operation case L_{ess}^{remov}:

$$L_{base}^{remov} = D_{base} \cdot L_{tot} \tag{15}$$

$$L_{ess}^{remov} = D_{ess} \cdot L_{tot} \tag{16}$$

$$y_{def} = L_{base}^{remov} - L_{ess}^{remov} \tag{17}$$

where D_{base} and D_{ess} are the damages incurred in the base and hybrid cases respectively.

- The future cost of turbine replacement is computed using the inflation rate (IR) as:

$$C_{fut} = C_{tot}^{r} * (1 + IR)^{y_{def}} \tag{18}$$

- Then, using the discount rate DR, present cost of turbine replacement is calculated:

$$C_{pres} = \frac{C_{fut}}{(1 + DR)^{y_{def}}} \tag{19}$$

- Finally, the benefit due to investment deferral is obtained:

$$B_{def} = C_{tot}^{r} - C_{pres} \tag{20}$$

- The total benefit due to hybrid operation B_{ess} is given as the sum of (14) and (20):

$$B_{ess} = B_{NPV} + B_{def} \tag{21}$$

3.0 Simulation and Case Studies

The analysis capabilities developed in the previous sections are put to the test by modeling the ESS-based hybridization of a real-world hydro turbine generator. The generating unit is a part of the Carmen-Smith power project located 71 miles east of Eugene on the upper McKenzie River in Oregon, USA. The facility comprises three dams, three reservoirs, and two power-generating plants. It is the largest utility-owned power source of Eugene Water and Electric Board (EWEB), a publicly owned water and electric utility. The plant specifications of both the generating units are presented in Table 2.

Table 2. Specifications of generating units at EWEB's Carmen-Smith hydropower facility.

Equipment	Manufacturer	Rating
Turbine	Allis Chalmers (Francis)	41.777MW / 56000HP / 240 RPM / 109 m
Generator	Westinghouse (Siemens)	55 MVA /11.5 kV / 0.95 PF
Governor	American Governor Co.	Digital electronic

(a) Normal operating head for turbine is 152.74 m

The machines, however, are operated at a turbine head and power output that is greater than the nameplate rating shown in Table 2. The operational head height is about 152.7 m, and the power output is 50 MW. In this section, the generating unit-2 is modeled and analyzed for the ESS-based hybridization. The power output data for this unit is provided by EWEB at the resolution of 3 seconds. Figure 13 shows the power output from unit-2 for one month. The power requirements on this unit change frequently and often become zero, resulting in the unit shutting down. For analysis, this utility-supplied power output is used as the dispatch signal for the controller.

As discussed earlier, the frequent changes in power requirements result in wear and tear of the generating unit. EWEB has a guide for the recommended operation of the two generating units at the Carmen facility as shown in Figure 28. Certain operating zones such as < 10 MW and > 45 MW are recommended to be avoided because they substantially decrease the life of the turbine. Combining these recommendations with the lack of information on the head of the hydropower plant during the power dispatch (as discussed in Section 2.1), we map fractions of operation of low part load, part load, BEP, and high load as shown in Table 3. This information is then used to calculate damage as explained in Section 2.1.

Table 3. Damage classification categories defined for unit-2 based on operational recommendations from EWEB.

Damage Class	Load (MW)
Low part load	$\leq$5
Part load	$>$ 5 and $\leq$ 15
BEP	$>$ 15 and $\leq$ 40
High load	$>$ 40

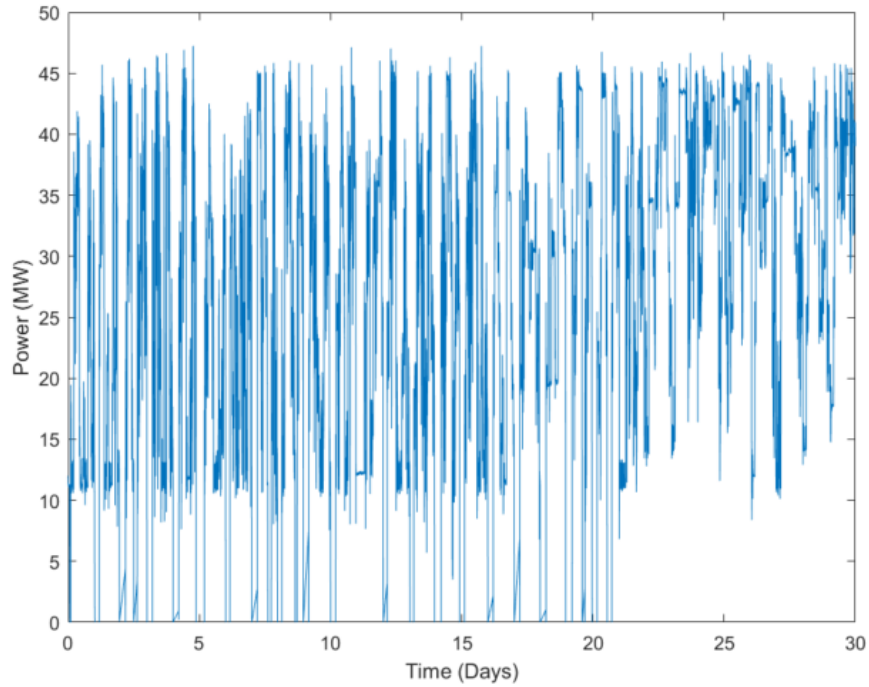

Figure 13. Power output of unit-2 for one month. The unit operation in the low part load region and frequent shutdowns/startups cause wear and tear.

3.1 Base Case

This case is set up to establish the baseline damage for the hydro turbine unit as it follows the dispatch signal provided by the utility. In the base case, the unmodified dispatch signal is used to determine the power output of the turbine. As discussed earlier, this dispatch signal ramps up and down rapidly and also results in the frequent shutdown of the unit; therefore, it is used to estimate baseline damage incurred in the unit. This is achieved by removing the hybrid controller and the ESS from Figure 9 to yield the setup shown in Figure 14. The specifications of the base case are presented in Table 4 and Table 5.

Figure 15 shows the plot of state variables i.e., x_{g1} through x_{g4}. As discussed in [22], in steady state, $\omega = \omega_{ref}$ so $x_{g1} = 0$. The gate position G and mechanical power P_m follow P_{ref}. Therefore in Figure 15, x_{g1} remains zero whereas other state variables correspond to system dynamics such as gate position and powers (electrical and mechanical). For comparison, the reference power P_{ref} is also plotted (i.e., the dispatch signal). The gate position, mechanical power, and electrical power follow the reference power signal P_{ref} as shown in Figure 16. There is a delay in the tracking of these signals that corresponds to the inertia of the turbine and generator.

The load disturbance signal is inserted to simulate the real-world load conditions or the load-generation imbalance. This is shown in Figure 15, where a large load imbalance can be seen at $t = 300$ sec. Due to this disturbance, the angular speed of the rotor and output frequency changes drastically. However, the load change is quickly damped by the governor, thereby bringing the angular frequency back to nominal. The damping action is demonstrated in Figure 17. As a result, the angular speed of the rotor and the output frequency of the machine is locked back to the reference frequency of 60 Hz.

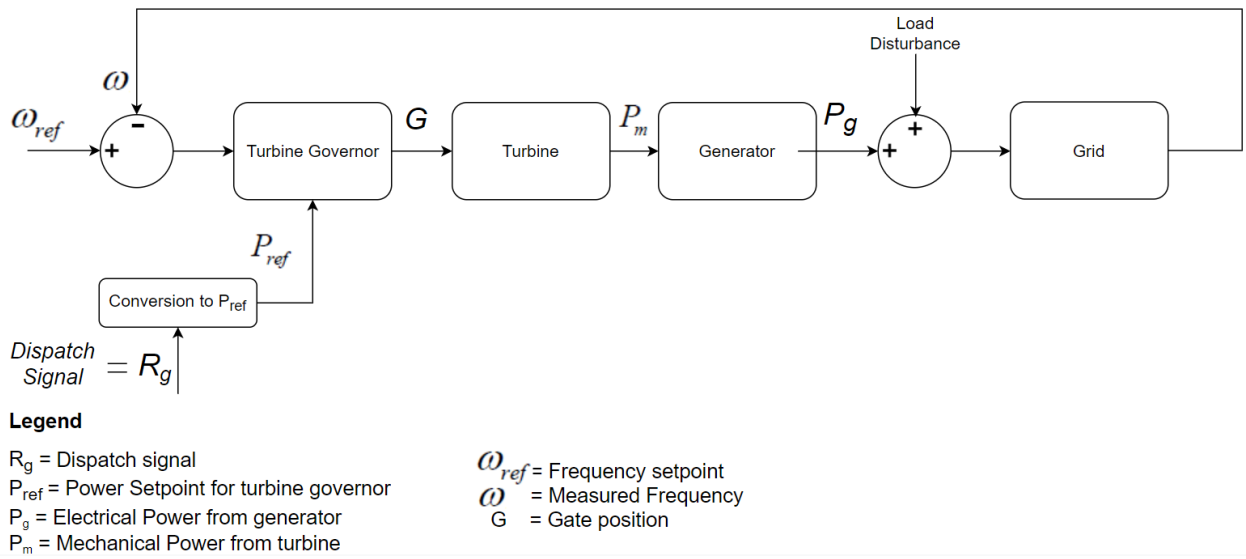

Figure 14. Setup for the base case simulation. EWEB's original dispatch signal drives the hydro turbine unit to provide an estimate of the baseline damage.

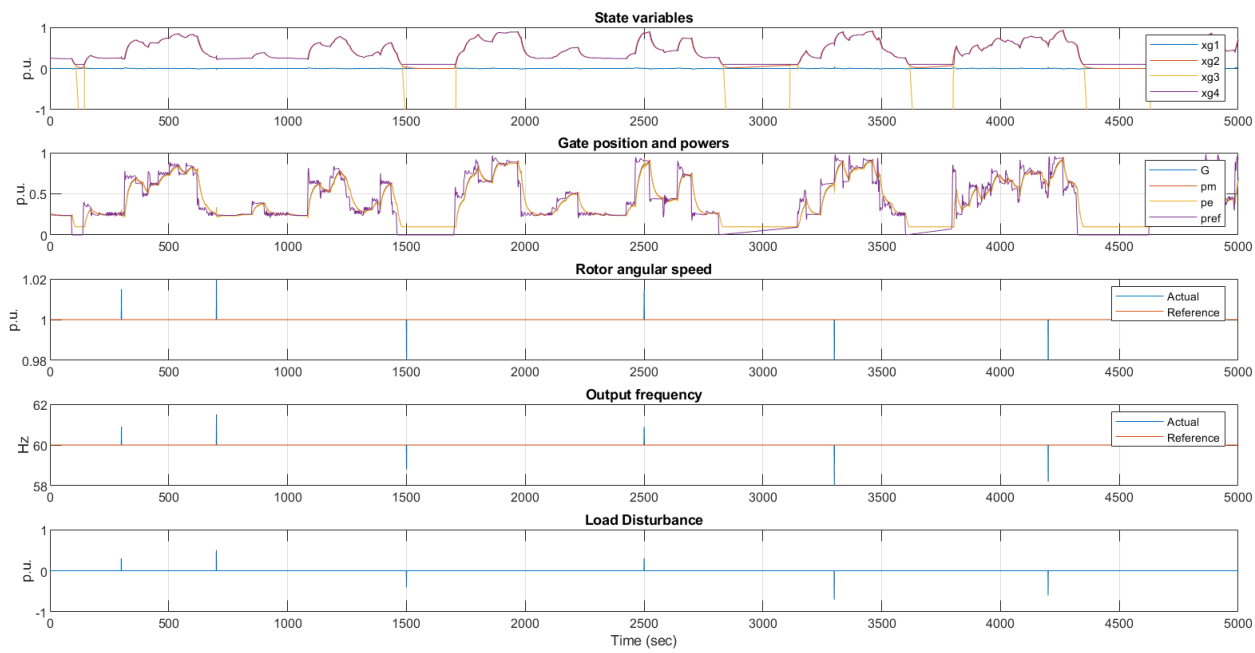

Figure 15. State variables in the base case simulation.

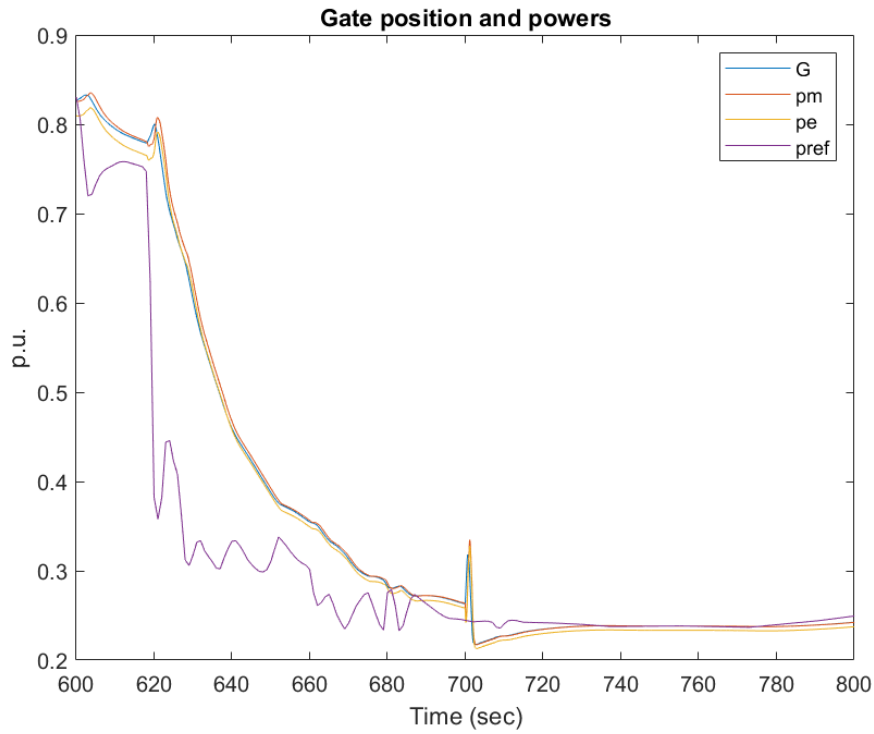

Figure 16. Electrical power (Pe), mechanical power (Pm), and gate position (G) follow the reference signal delayed by the inertia of the machine.

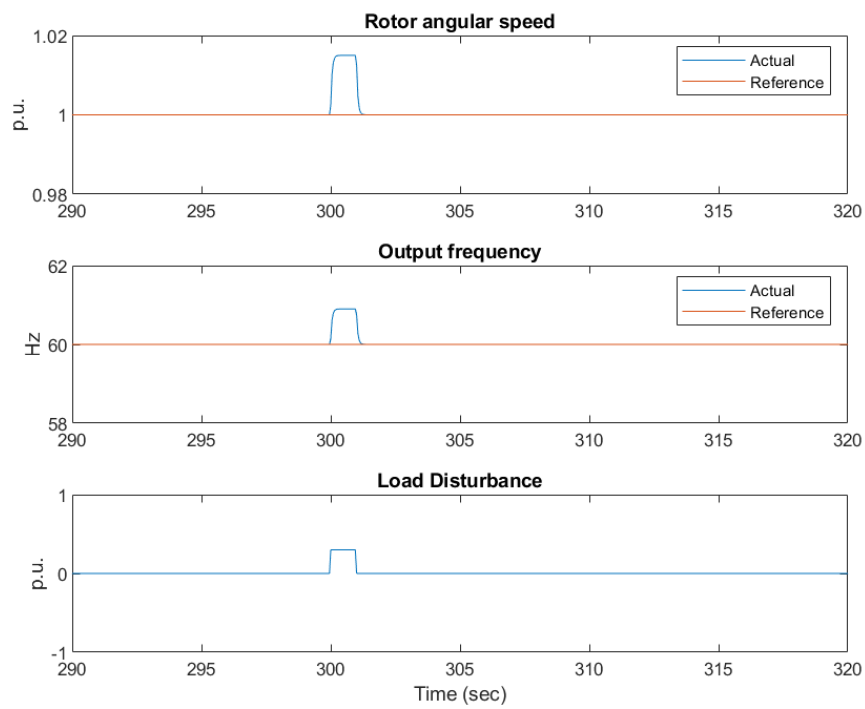

Figure 17. Load-generation imbalance to simulate the real-world loading conditions.

Using data from unit-2 in the Carmen-Smith hydro electric plant, damage classifications of

Table 3, and loss-of-life models discussed previously, the annual damage is calculated to be 0.098. Most of this damage occurs due to operation of the unit in the low part load region. The distribution of damage among other regions such as part load, BEP, high load, and start/stop is comparatively lesser as shown in Figure 18.

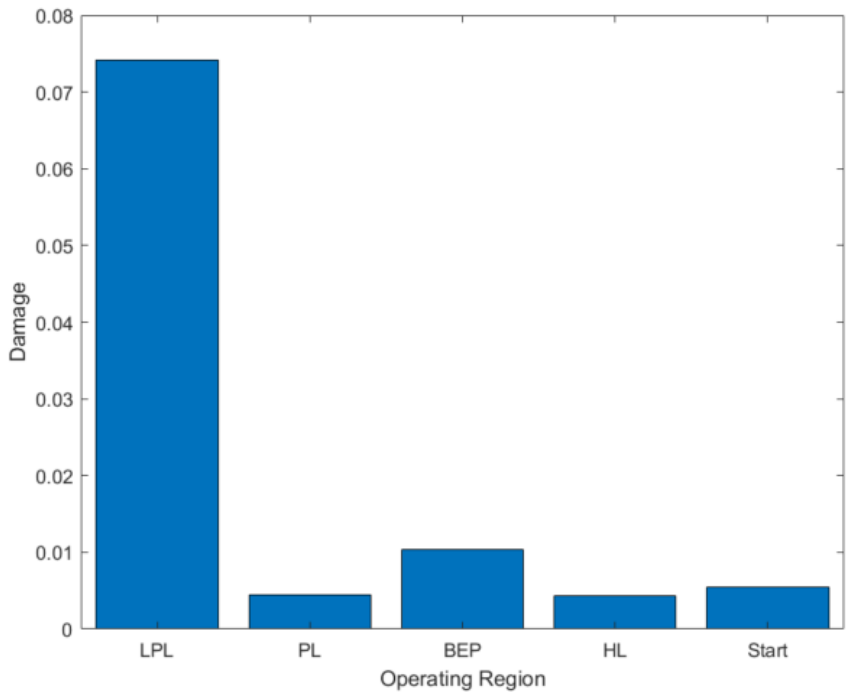

Figure 18. Breakdown of the damage incurred in base case simulation.

Table 4. Generator parameters

Generators parameters	Value (units)
Damping coefficient	2 (p.u.)
Inertial constant	0.05 (MW/MVA)
Armature resistance	0 (p.u.)
Leakage reactance	0 (p.u.)
d-axis synchronous reactance	1.05 (p.u.)
q-axis synchronous reactance	0.98 (p.u.)
q-axis transient reactance	0.36 (p.u.)
q-axis sub-transient reactance	0.13 (p.u.)
d-axis transient reactance	0.185 (p.u.)
d-axis sub-transient reactance	0.13 (p.u.)
Generator efficiency	98 (%)

Table 5. Turbine parameters

Turbine Parameters	Value (units)
K_i	1.5 (p.u.)
K_p	3 (p.u.)
G_{min}	0.1 (p.u.)
G_{max}	1 (p.u.)
T_g	0.2 (p.u.)
T_p	0.05 (p.u.)
T_w	1 (p.u.)
σ	0.04 (p.u.)
V_{min}	-0.1 (p.u.)
V_{max}	0.1 (p.u.)
Ω_0	1 (p.u.)

3.2 ESS-Based Hybridization with Fixed Battery size

In the hybrid operation case study, the utility dispatch signal is fed to the hybrid controller to generate two signals: a high-frequency energy-neutral signal for ESS and a low-frequency unidirectional signal for the hydro turbine generator. Then, the ESS control signal drives output that gets added to the output of the hydro turbine generator as shown previously in Figure 9. The specifications presented in Table 4 and Table 5 remain valid for this case study as well. Some additional specifications exclusive to this case are given in Table 6. The hybrid operation case reduces the damage for the turbine unit as it follows the modified dispatch signal generated by the hybrid controller. The battery used for this case is a 12.5 MW/25 MWh battery. The charge and discharge efficiencies for this battery are configured to be 0.96 and 0.95, respectively [34].

Table 6. Parameters for the hybrid controller.

Hybrid Controller Parameters	Value (units)
PID proportional gain	30
PID integration gain	0.01
PID derivative gain	0
Low-pass time constant	150 (sec)
High-pass time constant	6 (sec)

The utility dispatch signal is subdivided into two components when passed through the hybrid controller. The slower, ramp-limited signal shown in Figure 19 is used to dispatch the hydro turbine generator. The high-frequency, energy-neutral signal, shown in Figure 20, is fed

to the ESS. Note that the controller design is such that both signals, when added together, yield the original dispatch signal. Thus, the net output of the system at the point of common coupling equals the net output in the base case. The slower, ramp-limited signal of Figure 19 decreases the duration of the unit's operation in the low part load region. Moreover, it also avoids the frequent start and stops of the unit, thereby decreasing the overall damage. The dispatch signal for the ESS is kept energy-neutral to manage the inherent limitations of the ESS. The signal can ramp up and down frequently because most ESS technologies are capable of doing so.

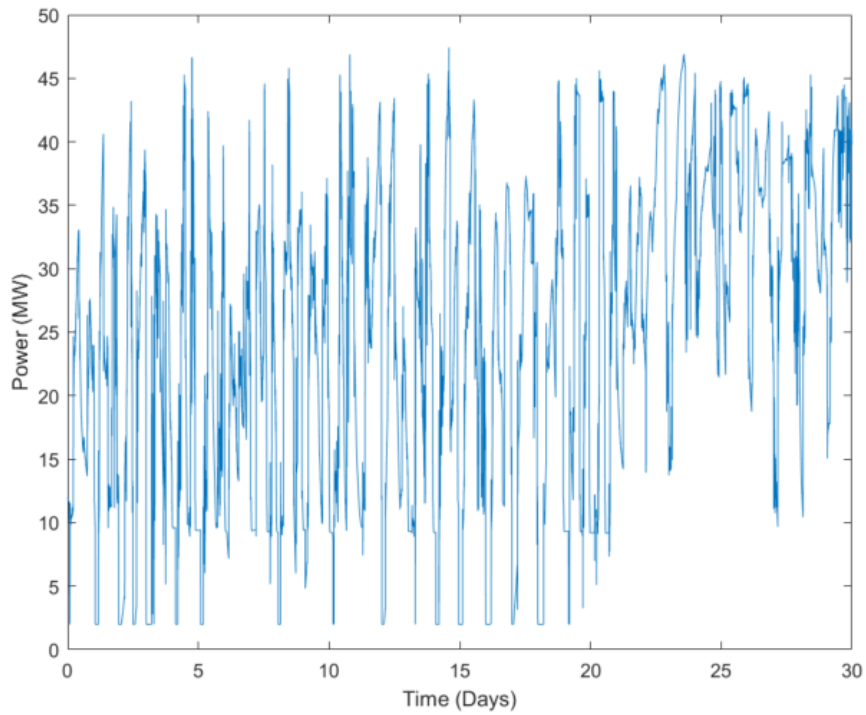

Figure 19. Ramp-limited, slowly varying dispatch signal for hydro turbine generator as generated by hybrid controller.

Figure 21 shows the plot of state variables (i.e., x_{g1} through x_{g4}) for the hybrid case. As discussed in the base case, x_{g1} remains zero whereas other state variables correspond to system dynamics such as gate position and powers (electrical and mechanical). Comparing plots to those in Figure 15 for the base case, it becomes obvious that the movement of the gate and subsequent changing of power is rather slow or smooth. Also, the generator is kept away from operation in the low part load region by specifying the minimum output in the hybrid controller and frequent start/stops are avoided. All this gets translated into lower damage for the hydro turbine generator. Since the inertial constants are kept the same as in the base case, the delay in tracking signals (i.e, gate signal, electrical and mechanical powers) with respect to P_{ref} is unchanged.

Thus, compared to the base case, the annual damage is reduced from 0.098 to 0.067 as shown in Figure 22. Due to the modified dispatch signal, the hydro turbine generator operates less in the low part load region when compared to the base case. It also avoids the frequent start and stops. Consequently, less damage is incurred in these two regions as shown in Figure 23. Since the unit operates mostly on the BEP and part load region, the damage in these two regions is slightly increased for the hybrid case when compared to the base case, but the overall damage is still less than the base case damage. Also, the start and stop damage is mitigated since the hybrid operation prevents the frequent starts and stops of the unit.

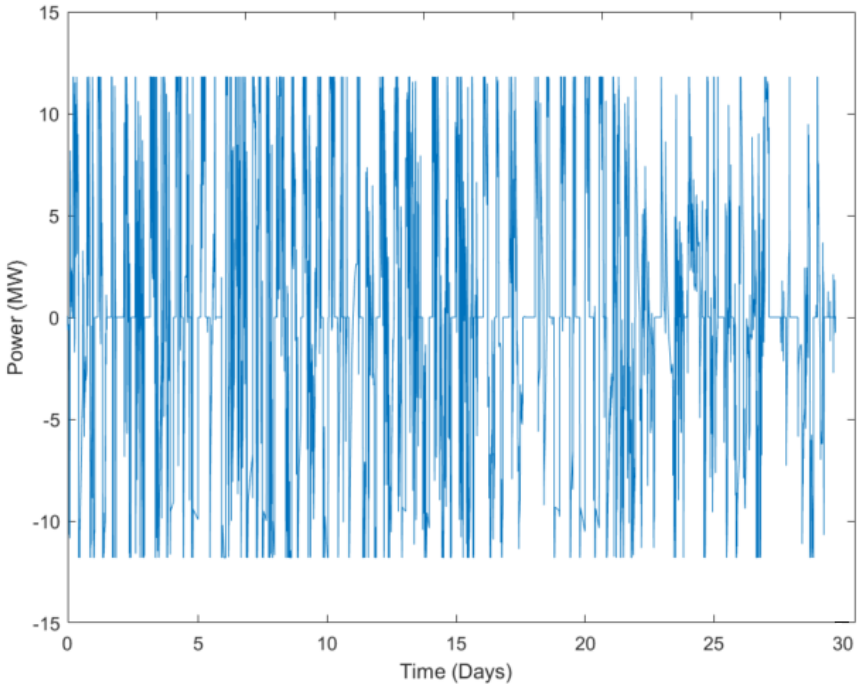

Figure 20. Energy-neutral, rapidly changing dispatch signal as generated by hybrid controller.

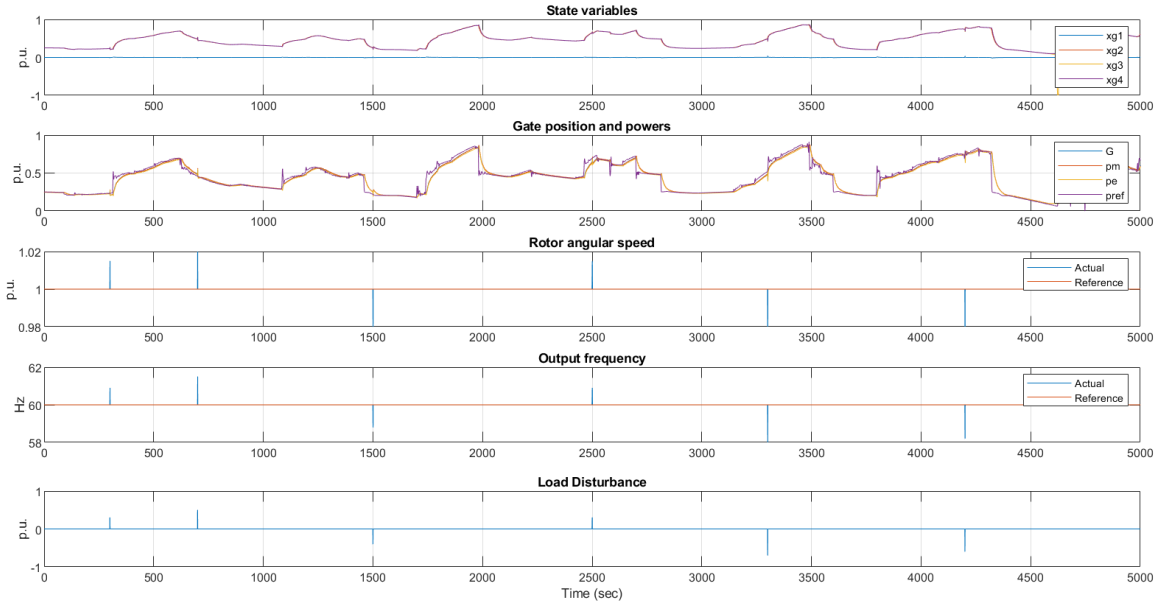

Figure 21. State variables in the hybrid case simulation.

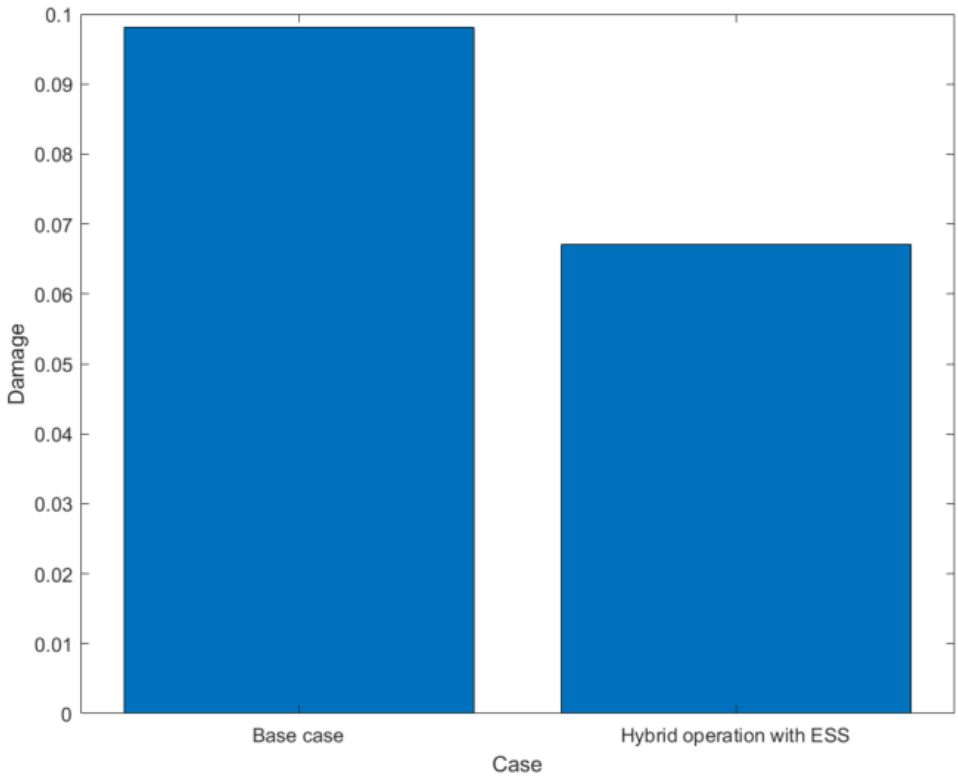

Figure 22. Comparing damage in hybrid case with the base case.

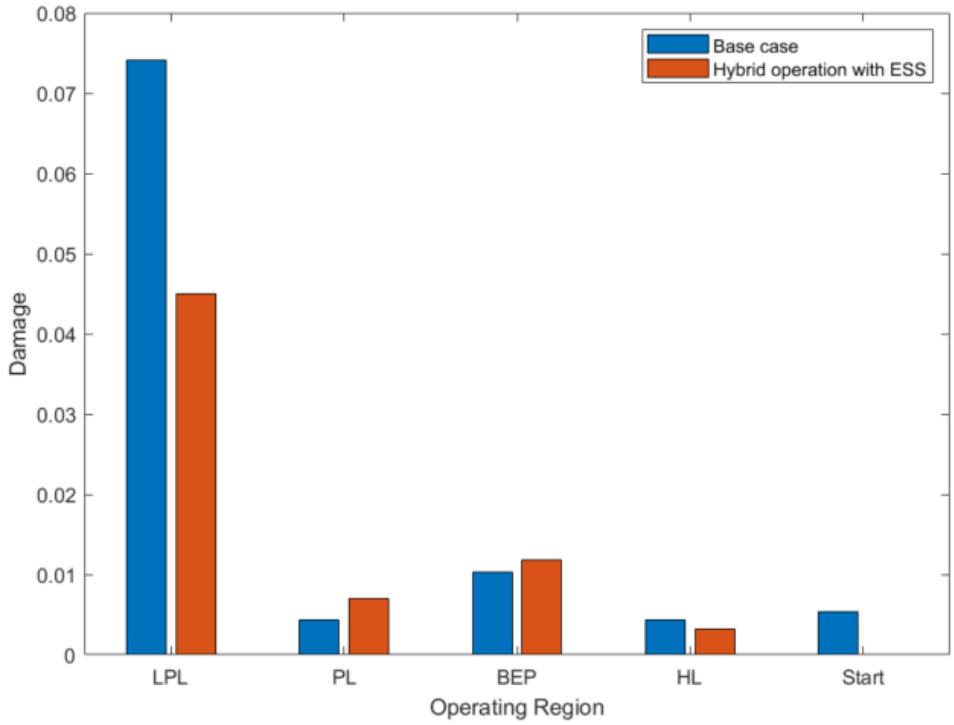

Figure 23. Comparing damage breakdown in hybrid case with the base case.

3.3 Sensitivity Analysis

The previous section discussed the capability of ESS to improve turbine lifetime. This section attempts to provide a generalized conclusion of such a capability by presenting the sensitivity analysis with respect to the storage size. This is done by changing the available peak power (MW) and energy capacity (MWh) in discrete steps while repeating the hybrid operation case study. For generalization, both peak power and energy capacity are normalized by the peak load of the original dispatched signal to obtain a p.u. interpretation. A 2-dimensional nexus is constructed by setting the resolution for peak power and energy capacity to be 5% (0.05 p.u.). For each point in this peak power-energy nexus, percentage damage reduction is computed due to the hybrid operation of the hydro turbine unit with the ESS. The results are shown in the 3-dimensional plot of Figure 24.

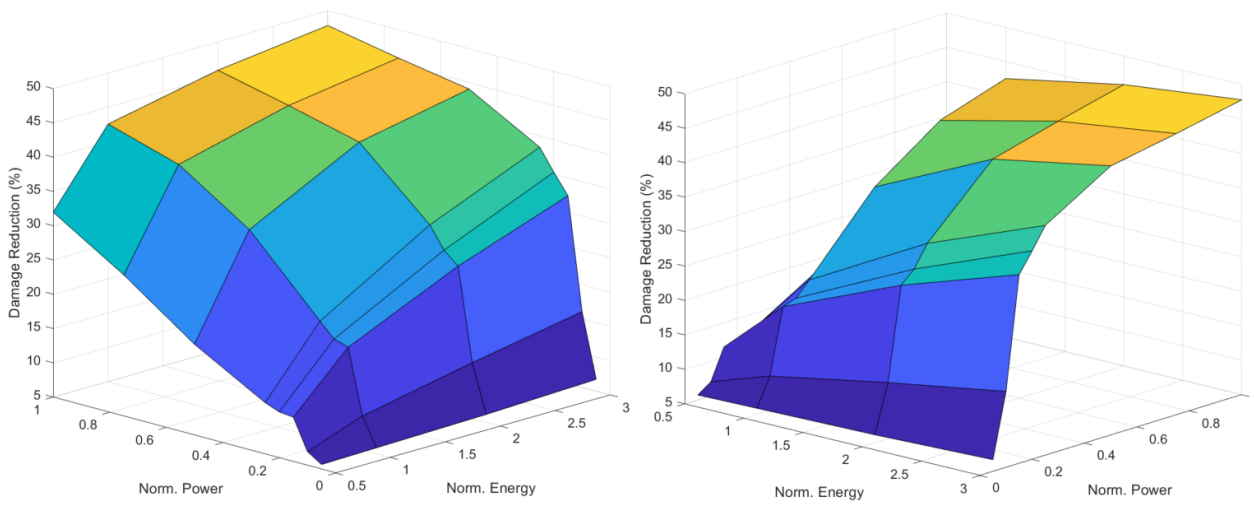

Figure 24. Percent damage reduction due to hybridization expressed as a function of normalized battery peak power and normalized energy capacity.

As a general trend, the percent damage reduction increases as the storage size increases. The maximum damage reduction is obtained with the ESS having a peak power capability equal to the load peak and having a duration of 3 hours, i.e., a 1 (p.u.)/3 (p.u.)h battery on this normalized scale. Reviewing Figure 24 for specific trends, both the power and energy capacity of the ESS impact damage reduction; however, their impact saturates after a certain ESS size. For example, damage reduction substantially increases until 1 (p.u.)h, but after that, the impact is lessened. This is due to the fact that in the proposed hybridization, most of the times ESS provides highly fluctuating power, and this operation is not energy-intensive (large spikes of power). However, to avoid the shutdown of the hydro generator and for the prevention of operation in the low part load region, energy requirements become much higher. Therefore, the energy requirements of ESS are greater than those in the regulation services, but less than what is required in capacity services. Considering the power requirements, the damage reduction steeply increases until 25% or 50% and then starts to saturate. This analysis demonstrates that for ESS-based hybridization, the main requirement is high power rather than high energy; large peak power is needed for short durations to mitigate adverse low part load conditions. However, note that the energy requirements are also not minimal, because to avoid start and stop conditions, the battery must have a certain energy capacity to keep the hydropower plant running.

3.4 Economic Analysis

To evaluate the economic benefits of ESS-based hybridization, an economic analysis is performed, assuming the parameters listed in Table 7. The cost of the turbine replacement is assumed to be $1.2M per MW. This is based on the estimates provided in [45], [3], [11], and [31]. Therefore, for the 42 MW unit under consideration, the total replacement cost becomes $50M. The annual inflation and discount rates are assumed to be 2% and 7.5%, respectively. These rates are essential in translating the costs from future years to the current year and vice versa. Finally, the total service life of the unit is assumed to be 50 years.

For the economic analysis, storage size is varied similar to the sensitivity analysis and damage is obtained for different scenarios. Using the calculated damage and input parameters of Table 7, the total benefit due to ESS-based hybridization is computed using (10)-(21). Figure 25 shows the total benefit from investment deferral and avoided maintenance for various ESS size scenarios. The trends seen in this analysis follow those observed for damage reduction. This is because the damage reduction directly translates into economic benefits. The benefits rise sharply as the ESS size in terms of power and energy capacity increases and then they start to saturate. Such analysis is useful in determining the optimal ESS size given the cost constraints.

For generalization, the total benefit is calculated over a range of turbine replacement costs and ESS sizes resulting in the 3-dimensional plot of Figure 26. The storage size is expressed in normalized MWs (using peak load of the original dispatched signal as the base) representing the peak power capability of the ESS. The turbine replacement cost is varied over the range of $1-2M per MW using $0.2M per MW as the step size. The energy capacity is kept equal to the power capacity, i.e., a 1-hour battery is assumed. In line with previous observations, Figure 26 shows that the total benefit steeply rises as the storage size is increased to about 25% of the peak load and then it almost evens out. For a fixed ESS size, the total benefit varies linearly with the turbine replacement cost. This is due to Equations (10) and (18) where the turbine replacement cost is expected to linearly impact the subsequently calculated costs and benefits.

Table 7. Economic analysis parameters.

Parameters	Value (units)
Turbine replacement cost	50M ($)
Discount rate	7.5 (%)
Inflation rate	2 (%)
System life	50 (years)

A benefit to cost ratio can be calculated by computing the capital cost of ESS installations. To this end, a cost of $1700/kW can be inferred from [29] for the Li-ion technology. Then a capital cost can be computed for different ESS sizes. The benefit-to-cost ratio is presented in Figure 27 for various ESS sizes and turbine replacement costs. It can be seen that the ratio generally stays less than 1.0 and increases with an increase in the turbine replacement cost. The ratio is minimized for large ESS sizes and low turbine costs and is maximized when the ESS power capacity is in the range of 15–25% on the normalized scale. This reemphasizes the fact that hybridization alone may not be sufficient to justify the economic merits of the ESS deployment. It should be stacked with other value streams to extract maximum benefit and therefore justify investment in large-scale ESS deployments.

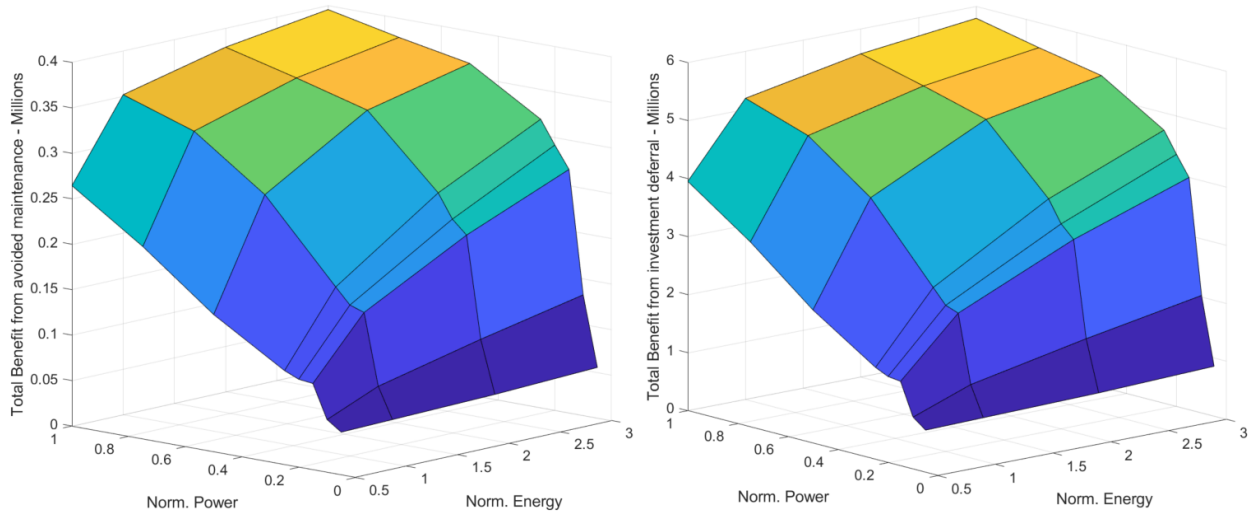

Figure 25. Total Benefit from avoided maintenance and total benefit from investment deferral.

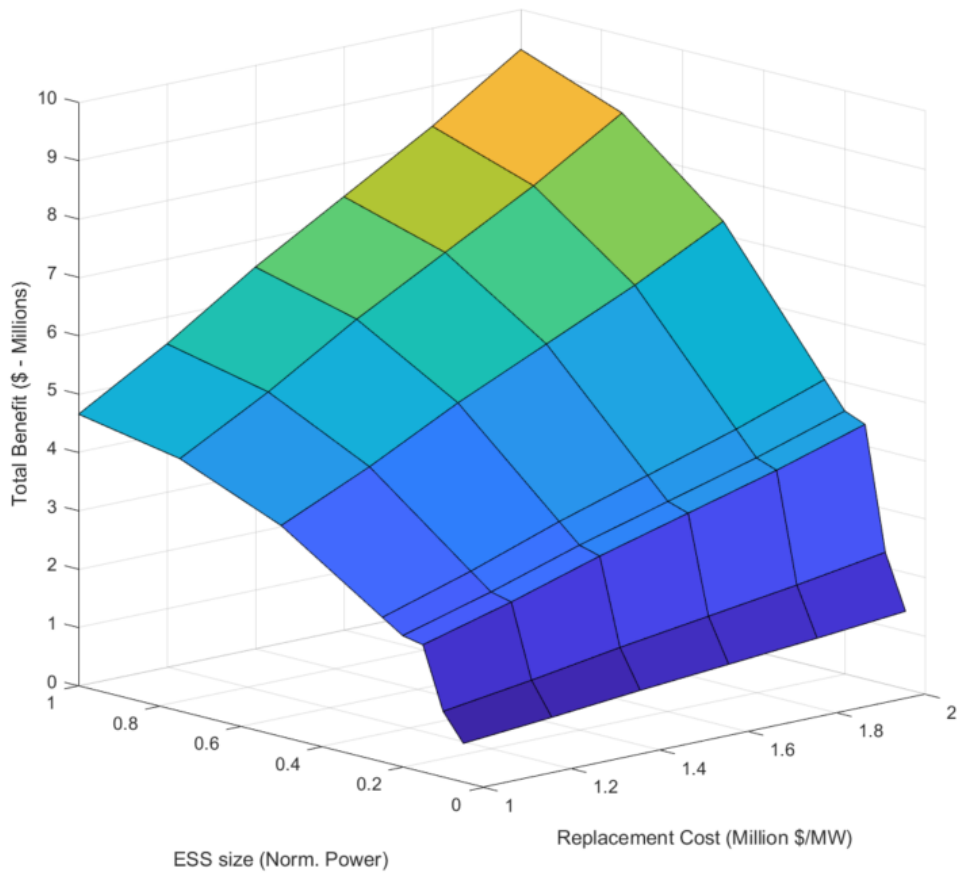

Figure 26. Total benefit from ESS-based hybridization over a range of turbine replacement costs and ESS sizes.

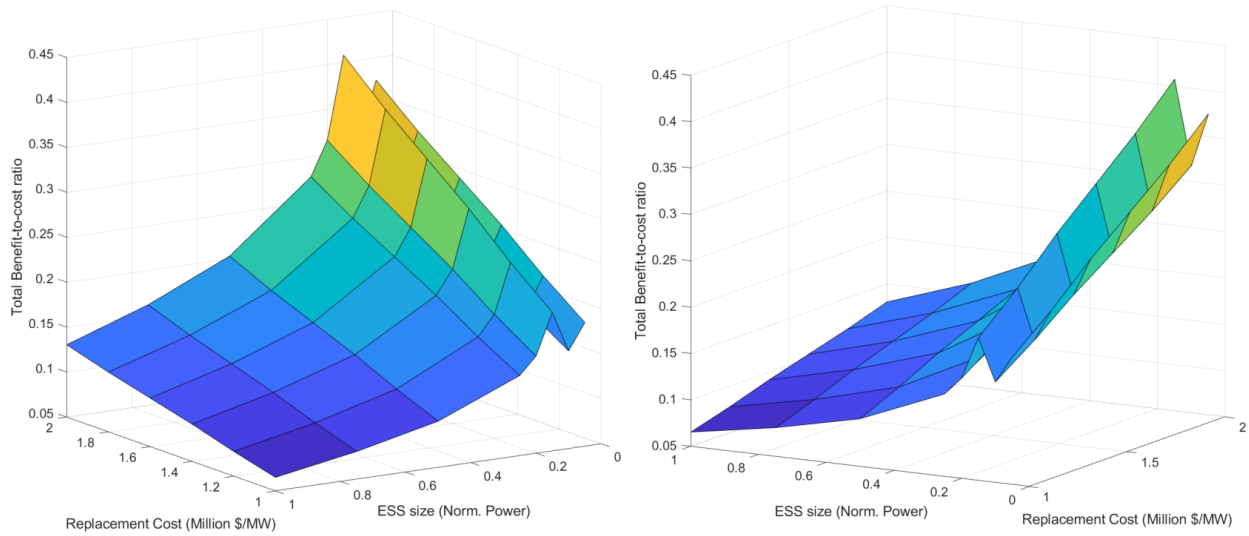

Figure 27. Benefit-to-cost ratio as a function of turbine replacement cost and ESS size.

3.5 Discussion of Results

The findings discussed in the previous sections show the benefits of ESS-based hybridization for hydropower units. These findings were discussed in light of various assumptions about unavailable data and relied on some simplification of methods; changes in assumptions and alternative modeling methodologies may bring further additions to the results of this section. To this end, the following are some discussion points that may be considered to further analyze the results.

- **Type of ESS**: Currently, there exists a generic SOC model to capture the efficiency of energy storage systems. Different storage types may be modeled to capture advanced storage capabilities, currently being explored in grid-scale applications. There are many types of grid-scale ESS technologies with different characteristics. They include electrochemical storage, PSH, thermal storage, compressed-air storage, electromechanical storage, and hydrogen storage systems. These types differ with respect to ramping rates, capital costs, technology readiness levels (TRLs), lifetime, and storage duration. Technologies such as electrochemical storage systems store energy in chemical form. They include Li-ion, lead-acid, redox flow, and other batteries. Among these, Li-ion provides a very high energy density and a longer life, whereas lead-acid has a high TRL but suffers from a poorer life. Electrochemical storage systems typically have higher ramping rates as compared to thermal storage systems, which store energy by heating or cooling a storage medium such as water or molten salt. Electromechanical storage systems such as flywheels take advantage of kinetic forces to store energy. They are capable of ramping up very quickly and providing very high energy for a brief period. The ramping rates of ESS technologies are directly related to the time constants of the hybrid controller. Also, the capital cost and TRL of certain technologies may cause the total deployment costs to outweigh the benefits of hybridization. Ultimately, the project is required to make decisions on the technology to be deployed in the ESS-based hybridization; hence, its specification and associated costs will impact the overall benefits.

- **Modeling aspects**: The loss-of-life models developed in this work may be influenced by the level of detail deployed in the model. That is, a high-fidelity modeling technique such as finite

element analysis [42] may bring further insight into the modeling and eventually yield different damage quantification. Similarly, power system models of generator and grid characteristics directly impact the results. Higher inertia of the generator would cause a higher delay in the tracking of gate position and power with respect to P_{ref}. Grid inertia determines the lag between the load-generation change and the subsequent impact on frequency.

- **Market Perspective**: The current analysis assumes that ESS is available in its entirety for the hybrid operation. In the real world, ESS may be bound to provide capacity or ancillary services to the grid. In that case, the ESS capacity available for the hybrid operation would be reduced, which would need to be factored into the decision-making process for the hybrid controller.

- **Policy Perspective**: Currently, no policy mandates or standard practices exist to connect ESS in the hybrid manner proposed in this study. To this end, policies and contractual agreements should be formulated and discussed, which will serve as guidance for future hybridization approaches. Further, existing DER interconnection standards may need to evolve, or new standards might be required, to accommodate ESS-based hybridization.

4.0 Conclusion and Recommendations

This work studies the potential of ESS deployment in the generation sector, compared to existing studies which primarily focus on T&D-oriented services. To this end, a new concept of operating ESS in combination with a hydropower generator is proposed. This effort focused on hydropower generating units, because they are required to provide higher flexibility than they have provided in the past. Although hydropower units can ramp up or down quickly compared to other assets such as thermal units, rapid load fluctuations inflict wear and tear on hydropower components. This damage translates into reduction of life and high maintenance costs. Therefore, in this report, ESS-based hybridization is discussed with an emphasis on loss of life and damage analysis. A hybridization strategy is proposed to provide relief such that the burden of highly variable dispatch of the hydropower unit is reduced by shifting that variability to the ESS.

The proposed strategy is embedded in a proof-of-concept framework incorporating an integrated model of a dynamic hydropower plant's turbine and its loss-of-life model. Using this framework, a configurable hybrid controller is proposed that hosts the hybridization strategy. The hydropower unit consists of individual models of the governor, turbine, and generator. The ESS is modeled as a power- and energy-limited asset without specific association with any technology. The controller contains error-correction mechanisms and blocks that generate the dispatch signals for the ESS and hydropower unit. Besides modeling of the physical assets, abstract models such as loss-of-life models, damage calculation models, and financial models are also provided. The proposed framework takes a utility dispatch signal as an input and runs as a closed-loop, self-correcting system. The dispatch signal is divided into two separate signals, with a smooth, slowly varying signal fed to the hydropower unit and the rapidly changing signal driving the ESS.

As discussed above, beyond the physical models, there exist abstract models that compute the loss of life and damage incurred by the hydropower unit. Once this damage is computed, the benefit of ESS-based hybridization is calculated using the financial models. The proposed framework is implemented as a self-contained package, and simulations are performed using real-world dispatch data from a utility. A real-world hydropower unit of 50 MW size is modeled in the simulations. Some of the results are summarized as:

- ESS-based hybridization is shown to reduce the total damage on the hydropower unit, using a control methodology that separates the high and low fluctuations from the dispatch signal (to be sent to ESS and hydropower plant, respectively). The damage reduction is because of avoiding operation in the low part load region and frequent start and stops. The maximum increase in the expected life of the hydro turbine is found to be 5% (when a 1 MW/3 MWh ESS is used on the normalized scale).

- The damage reduction is translated into direct benefits such as reduced maintenance requirements and indirect benefits such as investment deferrals. The average benefit with the assumption of $1.2/MW of turbine cost is found to be 3.6 million USD (when averaged over various ESS sizes).

- The extent of damage reduction varies with the power and energy capacity of the ESS. A sensitivity analysis provides an overview of the extent of damage reduction. An average damage reduction of 26% is observed due to ESS-based hybridization (when averaged over various ESS sizes).

The report also pinpointed the potential implications of variations in modeling parameters, data, and tools on the results of this study. The impacts of the type of ESS, market

participation, and policy directives are also discussed. Based on the presented framework, the following topics may be investigated in future work.

1. *Modeling Fidelity*: Results may be refined with higher-fidelity models for electrical and mechanical components of the hybridization concept of the paper, which includes (1) electrical frequency modeling using granular time resolution, electrical component models, and grid connections; (2) stress computation using a legacy complex surface stress simulator such as ANSYS or FEA; and (3) modeling verification and validation using historical data.

2. *Environmental*: Hydropower plants have a strong ecological footprint, which was not explored in this work. Future work may explore the impact of hybridization on the environment as well as whether the environmental impact imposes constraints on the hybridization technology.

3. *Optimization of Hybrid Resources*: The current modeling framework does not consider optimization based on projected future characteristics of ESS technologies and deployment conditions. Optimization problems may be explored in the future to answer questions such as sizing of the ESS technology based on its technology characterization, SOC management, and market opportunities (when the hybrid operation is co-optimized with other services).

4. *Co-optimization with Other Services*: Hybrid operation may be combined with other ESS services. A co-optimization-based strategy may allocate ESS capacity among various services to capture resulting value streams.

5. *Exploring Control Strategies*: It may be beneficial to explore other ESS hybridization and control strategies to yield improved performance. To this end, optimization, machine learning, or rule-based techniques may be explored to extend or completely overhaul the existing strategy.

5.0 Appendix

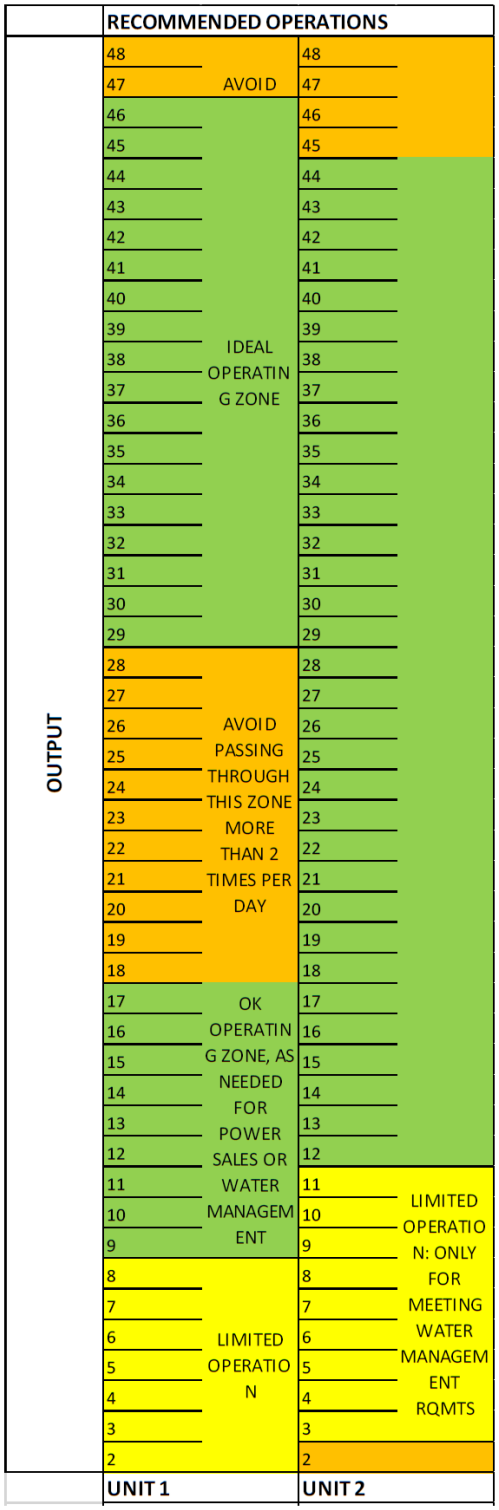

Figure 28. EWEB recommendations for operating generating units at the Carmen facility.

6.0 References

[1] Seyyed Mahdi Noori Rahim Abadi, Mahdi Davarpanah, Masoume Mahmoodi, Saman Nasiri, and Reza Bekhradian. Multiobjective optimal ders placement and sizing considering generator shaft fatigue. *IEEE Transactions on Power Systems*, 33(6):6787–6794, 2018.

[2] Jan Alam, Patrick Balducci, Kevin Whitener, and Steve Cox. Energy storage control capability expansion: Achieving better technoeconomic benefits at portland general electric's salem smart power center. *IEEE Power and Energy Magazine*, 18(2):69–80, 2020.

[3] Gaydaa AlZohbi. The cost of electromechanical equipment in a small hydro power storage plant. *Journal of Energy Systems*, 2(4):238–259, 2018.

[4] P Balducci, K Mongird, Md Jan Alam, D Wu, V Fotedar, V Viswanathan, A Crawford, Y Yuan, G Labove, S Richards, X Shane, and K Wallace. Washington clean energy fund grid modernization projects: Economic analysis. Technical report, Pacific Northwest National Lab.(PNNL), Richland, WA (United States), 2020.

[5] Patrick Balducci, Md Jan Alam, Tom McDermott, Vanshika Fotedar, Xu Ma, Di Wu, Bilal Ahmed Bhatti, Kendall Mongird, Bishnu Bhattarai, Alasdair Crawford, and Sumitrra Ganguli. Nantucket island energy storage system assessment. Technical report, Pacific Northwest National Lab.(PNNL), Richland, WA (United States), 2019.

[6] John Charles Butcher. A history of runge-kutta methods. *Applied numerical mathematics*, 20(3):247–260, 1996.

[7] Raymond H Byrne, Tu A Nguyen, David A Copp, Babu R Chalamala, and Imre Gyuk. Energy management and optimization methods for grid energy storage systems. *IEEE Access*, 6:13231–13260, 2017.

[8] André Coutu and Joel Chamberland-Lauzon. The impact of flexible operation on francis runners. *The International Journal on Hydropower & Dams*, 22(2), 2015.

[9] LD Douglas, TA Green, and RI A Kramer. New approaches to the agc nonconforming load problem. In *Conference Proceedings Power Industry Computer Application Conference*, pages 48–57. IEEE, 1993.

[10] J Endrenyi et al. Impact of maintenance strategy on reliability. *Final report by the IEEE/PES task force on impact of maintenance strategy on reliability of the reliability, risk and probability applications subcommittee*, 1999.

[11] Nline Energy. Preliminary analysis and concept study for replacement of hydroelectric facilities at the r.e. badger water filtration plant. Technical report, Tech. Rep., 2016.[Online]. Available: https://www.sfidwater.org/DocumentCenter/View/163/Hydroelectric-Preliminary-Concept-Study-PDF, 2016.

[12] Bloomberg New Energy Finance. 2019 long-term energy storage outlook. Technical report, Tech. Rep., 2019.[Online]. Available: https://about.bnef.com/blog/energy-storage-investments-boom-battery-costs-halve-next-decade/, 2019.

[13] ANDRITZ HYDRO GmbH. Modern hybrid solution for hydropower - hybatec. https://www.andritz.com/resource/blob/315340/8ae7977f51587508bc53d7ad587cffdf/hybatec-en-data.pdf, 2019.

[14] Salman Hajiaghasi, Ahmad Salemnia, and Mohsen Hamzeh. Hybrid energy storage system for microgrids applications: A review. *Journal of Energy Storage*, 21:543–570, 2019.

[15] Hans-Jörg Huth. Fatigue design of hydraulic turbine runners. 2005.

[16] PJM Interconnection. Implementation and rationale for pjm's conditional neutrality regulation signals. Technical report, Tech. Rep., Jan. 2017.[Online]. Available: https://www. pjm. com/ /media …, 2017.

[17] MC Jackson, SD Umans, RD Dunlop, SH Horowitz, and AC Parikh. Turbine-generator shaft torques and fatigue: part i-simulation methods and fatigue analysis. *IEEE Transactions on Power Apparatus and Systems*, (6):2299–2307, 1979.

[18] JJ Kauzlarich. The palmgren-miner rule derived. In *Tribology Series*, volume 14, pages 175–179. Elsevier, 1989.

[19] Muhammad Khalid, Abdollah Ahmadi, Andrey V. Savkin, and Vassilios G. Agelidis. Minimizing the energy cost for microgrids integrated with renewable energy resources and conventional generation using controlled battery energy storage. *Renewable Energy*, 97:646–655, 2016.

[20] D Kottick, M Blau, and D Edelstein. Battery energy storage for frequency regulation in an island power system. *IEEE transactions on energy conversion*, 8(3):455–459, 1993.

[21] Olivia Leitermann. *Energy Storage for Frequency Regulation on the Electric Grid*. PhD thesis, Massachusetts Institute of Technology, 2012.

[22] Wei Li. Hydro turbine and governor modeling and scripting for small-signal and transient stability analysis of power systems. *Master's degree project, KTH Royal Institute of Techonology, Stockholm, Sweden*, 2011.

[23] Chao-Tsung Ma and Chin-Lung Hsieh. Investigation on hybrid energy storage systems and their application in green energy systems. *Electronics*, 9(11), 2020.

[24] Marcelo Vinicius Magnoli. *Numerical simulation of pressure oscillations in large Francis turbines at partial and full load operating conditions and their effects on the runner structural behaviour and fatigue life*. PhD thesis, Technische Universität München, 2014.

[25] Pat March. Flexible operation of hydropower plants. *Electric Power Research Institute.(EPRI), Palo Alto, CA, Tech. Rep*, 2017.

[26] Patrick A March. Quantifying the maintenance costs associated with variable operating conditions. *HYDRO REVIEW*, 22(4):98–107, 2003.

[27] C Mende, W Weber, and U Seidel. Progress in load prediction for speed-no-load operation in francis turbines. In *IOP Conference Series: Earth and Environmental Science*, volume 49, page 062017. IOP Publishing, 2016.

[28] Milton A Miner. Cumulative damage in fatigue. 1945.

[29] Kendall Mongird, Vilayanur V Viswanathan, Patrick J Balducci, Md Jan E Alam, Vanshika Fotedar, V S Koritarov, and Boualem Hadjerioua. Energy storage technology and cost characterization report. Technical report, Pacific Northwest National Lab.(PNNL), Richland, WA (United States), 2019.

[30] Mostafa H. Mostafa, Shady H.E. Abdel Aleem, Samia G. Ali, Ziad M. Ali, and Almoataz Y. Abdelaziz. Techno-economic assessment of energy storage systems using annualized life cycle cost of storage (lccos) and levelized cost of energy (lcoe) metrics. *Journal of Energy Storage*, 29:101345, 2020.

[31] Navigant. Levelized cost of electricity for various power and energy efficiency options. https://www.hydro.org/waterpower/why-hydro/affordable/, 2009.

[32] U.S. Department of Energy. Energy storage grand challenge: Energy storage market report. Technical report, Tech. Rep., 2020.[Online]. Available: https://www.energy.gov/energy-storage-grand-challenge/downloads/energy-storage-market-report-2020, 2020.

[33] Bureau of Reclamation. Reclamation - managing water in the west. hydrogenerator start/stop costs. Technical report, U.S. Department of the Interior (United States), 2014.

[34] Michael Penev, Chad Hunter, and Joshua D Eichman. Energy storage: Days of service sensitivity analysis. Technical report, National Renewable Energy Lab.(NREL), Golden, CO (United States), 2019.

[35] DCH Prowse, P Koskela, TA Grove, and LR Larson. Experience with joint agc regulation. *IEEE transactions on power systems*, 9(4):1974–1979, 1994.

[36] Ernest Rabinowicz, RH McEntire, and B Shiralkar. A technique for accelerated life testing. 1970.

[37] CW Ross. Error adaptive control computer for interconnected power systems. *IEEE Transactions on Power Apparatus and Systems*, (7):742–749, 1966.

[38] Tetsuo Sasaki, Toshihisa Kadoya, and Kazuhiro Enomoto. Study on load frequency control using redox flow batteries. *IEEE Transactions on Power Systems*, 19(1):660–667, 2004.

[39] U Seidel, C Mende, B Hübner, W Weber, and A Otto. Dynamic loads in francis runners and their impact on fatigue life. In *IOP conference series: earth and environmental science*, volume 22, page 032054. IOP Publishing, 2014.

[40] Andreas Nilssen Skorpen. Impact from flexible operations on high head francis turbines. Master's thesis, NTNU, 2018.

[41] Tadeusz Stolarski, Yuji Nakasone, and Shigeka Yoshimoto. *Engineering analysis with ANSYS software*. Butterworth-Heinemann, 2018.

[42] Barna Szabó and Ivo Babuška. *Finite element analysis*. John Wiley & Sons, 1991.

[43] Alexandre Trudel, M Turgeon, and I Lanctôt. Recent trends in the design of hydropower components subjected to cycling and fatigue; towards improved technical design specifications. In *Hydrovision international conference*, 2017.

[44] Thomas Welte. Deterioration and maintenance models for components in hydropower plants. 2008.

[45] Adam Witt, Boualem Hadjerioua, Rocio Uría-Martínez, and NA Bishop Jr. Evaluation of the feasibility and viability of modular pumped storage hydro (m-psh) in the united states. *ORNL/TM-2015/559, Oak Ridge National Laboratory, Oak Ridge, Tennessee*, 2015.